Table 1
Sensitivities of $SHIV_{89.6P}$ and HIV-1_{LAI} to RTIs (AZT and 3TC) and PIs (LPV and RTV)

Virus	Cells	IC_{50} (μM) ± S.D.s[a]			
		AZT	3TC	LPV	RTV
$SHIV_{89.6P}$	M8166	0.007 ± 0.002	0.43 ± 0.0001	0.47 ± 0.09	0.44 ± 0.07
HIV-1_{LAI}	M8166	0.013 ± 0.001	0.31 ± 0.15	0.08 ± 0.01	0.03 ± 0.004

RTIs, reverse transcriptase inhibitors; AZT, zidovudine; 3TC, lamivudine. PIs, protease inhibitors; LPV, lopinavir; RTV, ritonavir.
[a] Data shown represent mean values (with standard deviations) derived from the result of two independent experiments conducted in duplicate. M8166 cells (5×10^3) were exposed to 100 $TCID_{50}$ of $SHIV_{89.6P}$ or HIV-1_{LAI} caltured in the presence of various concentrations of RTIs or PIs, and IC_{50}s were determined using the MTT assay on day 7 of culture.

increased during and after treatment compared with the pre-HAART level (49 ± 16 vs. 99 ± 26 per μl in mean $CD4^+$ count ± S.D., $P = 0.002$, 221 ± 81 vs. 392 ± 108 per μl in mean $CD8^+$ count ± S.D., $P = 0.01$) (Fig. 1A). At week 38, when HAART was initiated, the plasma viral load in MM260 was 3.4×10^4 copies/ml, and the proviral DNA was 6.8×10^4 copies/μg DNA. After commencement of HAART, the viral RNA in the plasma declined to below the threshold of detection within 3 weeks post HAART. On the other hand, proviral DNA remained detectable under the treatment though a continuous decline in the level was observed at 9 weeks post HAART (Fig. 1B).

In the low viral load monkey, MM242, the $CD4^+$ cell numbers were maintained over 400 per μl before HAART but the macaque also showed a decline in $CD4^+$ but not $CD8^+$ T cell counts before HAART compared with the pre-infection level (2152 ± 542 vs.

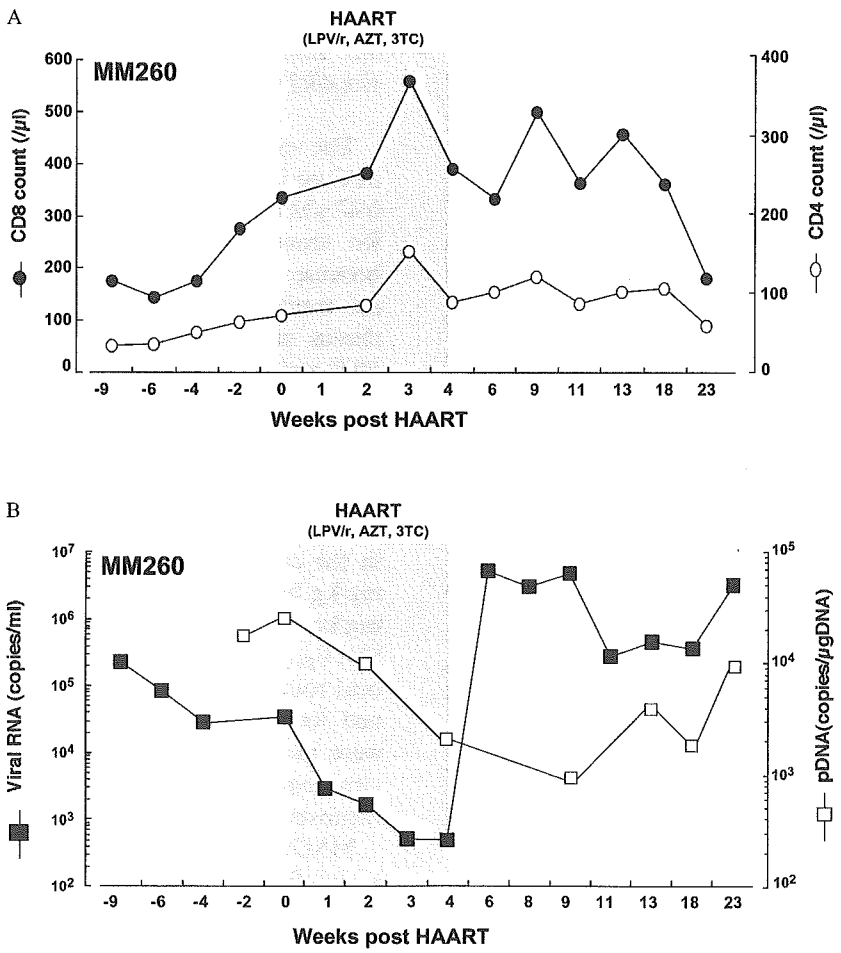

Fig. 1. Analyses of $SHIV_{89.6P}$-infected rhesus macaque MM260 treated with LPV/r, AZT and 3TC for 4 weeks by the oral route. $CD4^+$ and $CD8^+$ T cell counts (A), and plasma viral load and proviral DNA copy number (B) assessed within the peripheral blood are shown. The treatment period is shaded.

577±139 per μl in mean $CD4^+$ count±S.D., $P<0.001$, 761±248 vs. 447±188 per μl in mean $CD8^+$ count± S.D., $P=0.09$). However, there was no significant difference between pre- and after HAART in $CD4^+$ and $CD8^+$ T cell counts (577±139 vs. 569±180 per μl in mean $CD4^+$ count±S.D., $P=0.93$, 447±188 vs. 385±159 per μl in mean $CD8^+$ count±S.D., $P=0.52$) (Fig. 2A). The plasma viral load in MM242 was detectable at one point (9 weeks before HAART) before the treatment, and was never detected during and after treatment. The proviral DNAs in MM242 were also low (<300–1590 copies/μg DNA), and was maintained below the threshold of detection after the discontinuation of HAART (Fig. 2B).

3.3. Analysis of $CD8^+Ki67^+$ T cells in $SHIV_{89.6P}$-infected macaques with HAART

We determined Ki67-positive $CD8^+$ T cells in $SHIV_{89.6P}$-infected and uninfected monkeys using four-color flow cytometry analysis (Sachsenberg et al., 1998; Sodora et al., 2002). In the $SHIV_{89.6P}$-infected animal with a high viral load, MM260, growth fraction (percentage of Ki67) of $CD8^+$ T cells (10.98%) before HAART was higher than the value in the uninfected monkey (1.07%). The Ki67-positive $CD8^+$ T cells in MM260 were increasing during HAART, especially in the $CD45RA^-$ (CD8 memory) subset. After the discontinuation of HAART, the percentage of $CD8^+Ki67^+$ subset declined to the pre-treatment level (Fig. 3A and B). In MM242, the percentage of $CD8^+Ki67^+$ subset at 4 weeks before HAART was comparable to that of the uninfected monkey (0.83 vs. 0.85%). Ki67 levels were elevated after the treatment and were maintained at a high level until 18 weeks post HAART (7.95%). $CD8^+CD45RA^+Ki67^+$ T cells in MM242 increased after HAART, however, the $CD8^+CD45RA^-Ki67^+$ T cells were also increasing and overcame the percentage of $CD8^+CD45RA^+Ki67^+$ T cells by 13 weeks post HAART (Fig. 3C and D). We also determined Ki67 positivity in $CD8^+CD56^+$ T cells in MM242 at pre- and post-HAART. The percentages of $CD56^+Ki67^+$ were 0% and 0.05% in the $CD8^+$ T cell population at pre- (−3 weeks) and post- (22 weeks) HAART, respectively, using flow cytometry analysis. There

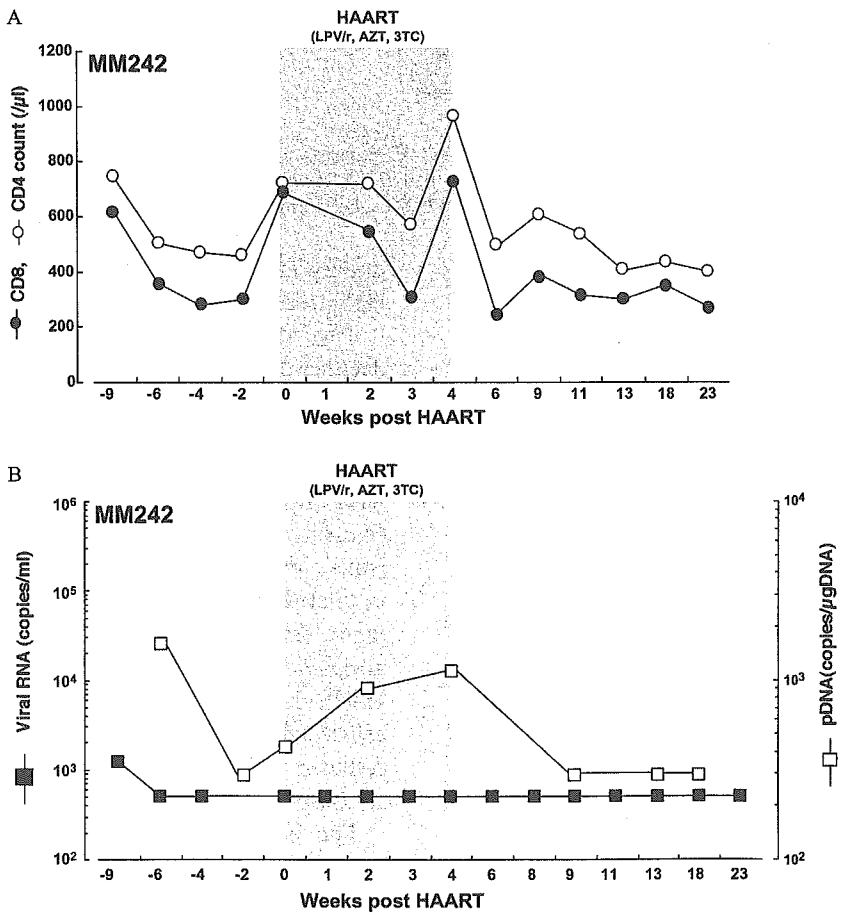

Fig. 2. Analyses of $SHIV_{89.6P}$-infected rhesus macaque MM242 treated with LPV/r, AZT and 3TC for 4 weeks by the oral route. $CD4^+$ and $CD8^+$ T cell counts (A), and plasma viral load and proviral DNA copy number (B) assessed within the peripheral blood are shown. The treatment period is shaded.

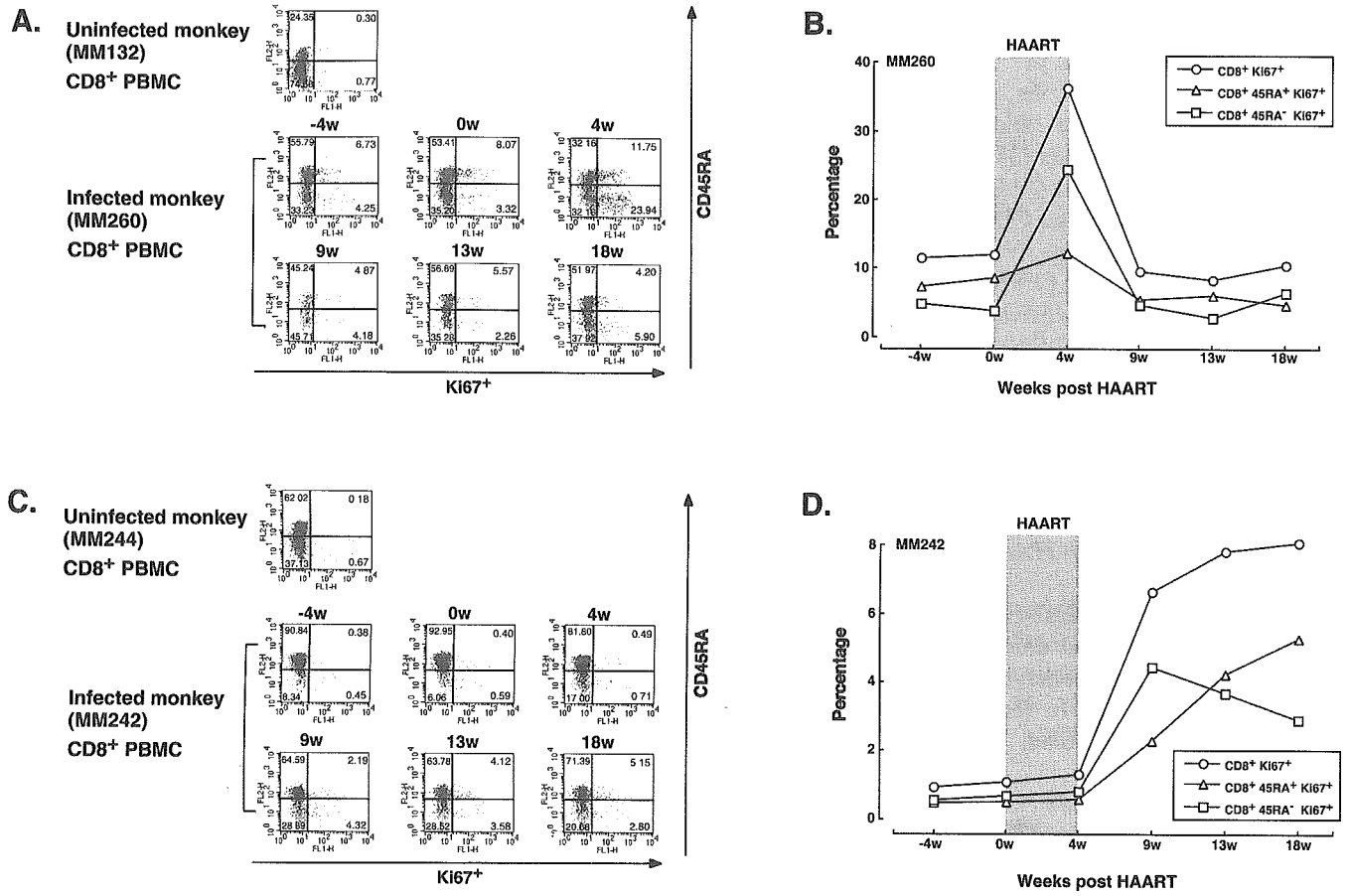

Fig. 3. Flow cytometry analysis of $CD8^+CD45RA^+$ cells stained with Ki-67. Expression of Ki-67 (percentage) in $CD8^+$ T cells of a control monkey and a $SHIV_{89.6P}$-infected monkey MM260 (A) and MM242 (C) at −4, 0, 4, 9, 13, 18 weeks post HAART. The percentage of cells expressing Ki-67 and CD45RA in $CD8^+$ T cells is depicted for MM260 (B) and MM242 (D). The treatment period is shaded.

seemed to be little contribution of $CD8^+$ NK cells in our data on $CD8^+Ki67^+$ T cells.

4. Discussion

This is apparently the first demonstration that the model of chronically $SHIV_{89.6P}$ infected-monkey with a therapeutic design recommended for humans by the oral route is feasible. The reduction of viral load and proviral DNA during the chronically infected stage was observed in treated animals together with the increase of CD4 and CD8 positive T lymphocyte subsets, especially memory T cells. Moreover, in both macaques, the percentages of $CD8^+Ki67^+$ cells increased during HAART, especially in the low viral load monkey (MM242) and the subset was maintained at a high percentage until 18 weeks post HAART. In CD4 positive T cells, $Ki67^+$ cells were also increased until 18 weeks post HAART in MM242 (data not shown). These results suggest that the oral treatment system in chronically infected-monkeys may prove to be a useful tool for monitoring immunological changes undergoing novel antiviral strategies with the usual anti-HIV treatment regimen.

The recent use of HAART has indicated that the decline of viral load in plasma and tissues generally results in an increase of T cell counts in peripheral blood (Autran et al., 1997; Evans et al., 1998; Mezzaroma et al., 1999; Pakker et al., 1998), which is often associated with improvement in clinical and immunological status (Autran et al., 1997; Evans et al., 1998). The mechanism(s) involved in such a peripheral T cell repopulation is unclear and may reflect the contribution of T cells from lymphoid tissues as a consequence of the reduced antigenic stimulation (Autran et al., 1997; Pakker et al., 1998), the capability for de novo production of naïve T cells (Hellerstein et al., 1999), and a decreased rate of T cell loss, which may reflect a reduced T cell susceptibility to apoptotic stimuli (Gougeon et al., 1999).

The issue of T lymphocyte turnover is central to understanding of HIV-1 pathogenesis (Antia and Halloran, 1996). Sachsenberg et al. estimated that HIV-1-infected individuals had a mean 6-fold increase in $CD8^+$T cell turnover, whereas the mean turnover of $CD4^+$T cells only increased by 2-fold (Sachsenberg et

al., 1998). The higher turnover of $CD8^+$T cells reflects the inversion of the $CD4^+/CD8^+$ ratio in HIV-1-infected patients (Chun et al., 2002; Margolick et al., 1995). In those studies, differences in $CD4^+$ and $CD8^+$T cell turnover also depend on stage of the disease, as defined by $CD4^+$ T cell counts.

$CD8^+$ T cell counts and the percentage of $CD8^+CD45RA^-$ (memory) T cells in both chronically infected macaques increased after oral route treatment. These findings were usually seen in clinical cases at the beginning of HAART (Autran et al., 1997; Badley et al., 1999; Pakker et al., 1998). However, the majority of $CD8^+$ memory cells increased following HAART was not considered as HIV-specific T cells. Because levels of HIV-specific effect CTL in treatment individuals fell (median half-life, 45 days) while viral RNA remained undetectable (Ogg et al., 1999). It is conceivable that following HAART reduction of apoptosis in $CD8^+$ memory cells may lead to an increase in the population. Our finding in infected monkeys with HAART was very similar to the kinetic of $CD8^+$ T cells after treatment of humans. The experiment presented in this report may provide an animal model of the phenomenon observed in HIV infected patients. Further analysis of repopulated $CD8^+$ T cells would be of interest because HIV-1 specific $CD8^+$ T cells during chronic infection in humans are enriched in cells of the $CD28^-CD27^+$ phenotype that proliferate but do have reduced CTL activity (Appay et al., 2002). Whether or not the proliferating $CD8^+$ T cells in our macaques given HAART are cells of this phenotype will need to be determined.

The plasma HIV-1 RNA is widely considered to be a direct indicator of the overall level of HIV-1 expression in infected individuals. However, it was reported that the concentration of HIV-1 DNA in PBMC complements the HIV-1 RNA load in plasma in predicting the clinical outcome of HIV-1 disease (Kostrikis et al., 2002). In our findings, especially in MM242 with a low plasma $SHIV_{89.6P}$ RNA load, the proviral DNA also may be an indicator of residual replication when plasma RNA loads were undetectable as seen in HIV-1 infected patients (Kostrikis et al., 2002; O'Doherty et al., 2002).

These monkey model given antiviral drugs by the oral route will enable the investigation of immunological changes during novel drug testing and also antiviral strategies combined with HAART.

Acknowledgements

We thank K. Yoshida and N. Shirai for excellent technical assistance and Dr A. Koito for helpful comments on the manuscript. This work was supported in part by Research for Scientific Research Grant of the Japan Society for the Promotion of Science (#14021099), a Grant-in-Aid for Scientific Research (Priority Areas) from the Ministry of Education, Culture, Sports, Science, and Technology of Japan (Monbu-Kagakusho)(#14570422).

References

Antia, R., Halloran, M.E., 1996. Recent developments in theories of pathogenesis of AIDS. Trends Microbiol. 4 (7), 282–285.

Appay, V., Dunbar, P.R., Callan, M., Klenerman, P., Gillespie, G.M., Papagno, L., Ogg, G.S., King, A., Lechner, F., Spina, C.A., Little, S., Havlir, D.V., Richman, D.D., Gruener, N., Pape, G., Waters, A., Easterbrook, P., Salio, M., Cerundolo, V., McMichael, A.J., Rowland-Jones, S.L., 2002. Memory $CD8^+$ T cells vary in differentiation phenotype in different persistent virus infections. Nat. Med. 8 (4), 379–385.

Autran, B., Carcelain, G., Li, T.S., Blanc, C., Mathez, D., Tubiana, R., Katlama, C., Debre, P., Leibowitch, J., 1997. Positive effects of combined antiretroviral therapy on $CD4^+$ T cell homeostasis and function in advanced HIV disease. Science 277 (5322), 112–116.

Badley, A.D., Parato, K., Cameron, D.W., Kravcik, S., Phenix, B.N., Ashby, D., Kumar, A., Lynch, D.H., Tschopp, J., Angel, J.B., 1999. Dynamic correlation of apoptosis and immune activation during treatment of HIV infection. Cell Death Differ. 6 (5), 420–432.

Carrillo, A., Stewart, K.D., Sham, H.L., Norbeck, D.W., Kohlbrenner, W.E., Leonard, J.M., Kempf, D.J., Molla, A., 1998. In vitro selection and characterization of human immunodeficiency virus type 1 variants with increased resistance to ABT-378, a novel protease inhibitor. J. Virol. 72 (9), 7532–7541.

Chun, T.W., Justement, J.S., Pandya, P., Hallahan, C.W., McLaughlin, M., Liu, S., Ehler, L.A., Kovacs, C., Fauci, A.S., 2002. Relationship between the size of the human immunodeficiency virus type 1 (HIV-1) reservoir in peripheral blood $CD4^+$ T cells and $CD4^+$:$CD8^+$ T cell ratios in aviremic HIV-1-infected individuals receiving long-term highly active antiretroviral therapy. J. Infect. Dis. 185 (11), 1672–1676.

Clapham, P.R., Weiss, R.A., Dalgleish, A.G., Exley, M., Whitby, D., Hogg, N., 1987. Human immunodeficiency virus infection of monocytic and T-lymphocytic cells: receptor modulation and differentiation induced by phorbol ester. Virology 158 (1), 44–51.

Clavel, F., Guetard, D., Brun-vezinet, F., Chamaret, S., Rey, M.A., Santos-ferreira, M.O., Laurent, A.G., Dauguet, C., Katlama, C., Rouzioux, C., 1986. Isolation of a new human retrovirus from West African patients with AIDS. Science 233 (4761), 343–346.

Endo, Y., Igarashi, T., Nishimura, Y., Buckler, C., Buckler-White, A., Plishka, R., Dimitrov, D.S., Martin, M.A., 2000. Short- and long-term clinical outcomes in rhesus monkeys inoculated with a highly pathogenic chimeric simian/human immunodeficiency virus. J. Virol. 74 (15), 6935–6945.

Enose, Y., Ui, M., Miyake, A., Suzuki, H., Uesaka, H., Kuwata, T., Kunisawa, J., Kiyono, H., Takahashi, H., Miura, T., Hayami, M., 2002. Protection by intranasal immunization of a nef-deleted, nonpathogenic SHIV against intravaginal challenge with a heterologous pathogenic SHIV. Virology 298 (2), 306–316.

Evans, T.G., Bonnez, W., Soucier, H.R., Fitzgerald, T., Gibbons, D.C., Reichman, R.C., 1998. Highly active antiretroviral therapy results in a decrease in $CD8^+$ T cell activation and preferential reconstitution of the peripheral $CD4^+$ T cell population with memory rather than naive cells. Antiviral Res. 39 (3), 163–173.

Gougeon, M.L., Lecoeur, H., Sasaki, Y., 1999. Apoptosis and the CD95 system in HIV disease: impact of highly active anti-retroviral therapy (HAART). Immunol. Lett. 66 (1–3), 97–103.

Haigwood, N.L., 1999. Progress and challenges in therapies for AIDS in nonhuman primate models. J. Med. Primatol. 28 (4–5), 154–163.

Hellerstein, M., Hanley, M.B., Cesar, D., Siler, S., Papageorgopoulos, C., Wieder, E., Schmidt, D., Hoh, R., Neese, R., Macallan, D., Deeks, S., McCune, J.M., 1999. Directly measured kinetics of circulating T lymphocytes in normal and HIV-1-infected humans. Nat. Med. 5 (1), 83–89.

Igarashi, T., Brown, C.R., Endo, Y., Buckler-White, A., Plishka, R., Bischofberger, N., Hirsch, V., Martin, M.A., 2001. Macrophage are the principal reservoir and sustain high virus loads in rhesus macaques after the depletion of $CD4^+$ T cells by a highly pathogenic simian immunodeficiency virus/HIV type 1 chimera (SHIV): implications for HIV-1 infections of humans. Proc. Natl. Acad. Sci. USA 98 (2), 658–663.

Kimura, T., Yoshimura, K., Nishihara, K., Maeda, Y., Matsumi, S., Koito, A., Matsushita, S., 2002. Reconstitution of spontaneous neutralizing antibody response against autologous human immunodeficiency virus during highly active antiretroviral therapy. J. Infect. Dis. 185 (1), 53–60.

Kostrikis, L.G., Touloumi, G., Karanicolas, R., Pantazis, N., Anastassopoulou, C., Karafoulidou, A., Goedert, J.J., Hatzakis, A., 2002. Quantitation of human immunodeficiency virus type 1 DNA forms with the second template switch in peripheral blood cells predicts disease progression independently of plasma RNA load. J. Virol. 76 (20), 10099–10108.

Le Grand, R., Clayette, P., Noack, O., Vaslin, B., Theodoro, F., Michel, G., Roques, P., Dormont, D., 1994. An animal model for antilentiviral therapy: effect of zidovudine on viral load during acute infection after exposure of macaques to simian immunodeficiency virus. AIDS Res. Hum. Retroviruses 10 (10), 1279–1287.

Le Grand, R., Vaslin, B., Larghero, J., Neidez, O., Thiebot, H., Sellier, P., Clayette, P., Dereuddre-Bosquet, N., Dormont, D., 2000. Post-exposure prophylaxis with highly active antiretroviral therapy could not protect macaques from infection with SIV/HIV chimera. AIDS 14 (12), 1864–1866.

Le Grand, R., Vaslin, B., Benlhassan, K., Thiebot, H., Dereuddre-Bosquet, N., Clayette, P., Dormont, D., 2002. Post-exposure prophylaxis with HAART in macaques exposed to pathogenic SIV or SHIV. XIV International AIDS Conference.

Li, J., Lord, C.I., Haseltine, W., Letvin, N.L., Sodroski, J., 1992. Infection of cynomolgus monkeys with a chimeric HIV-1/SIVmac virus that expresses the HIV-1 envelope glycoproteins. J. Acquired Immune Defic. Syndr. 5 (7), 639–646.

Maeda, K., Yoshimura, K., Shibayama, S., Habashita, H., Tada, H., Sagawa, K., Miyakawa, T., Aoki, M., Fukushima, D., Mitsuya, H., 2001. Novel low molecular weight spirodiketopiperazine derivatives potently inhibit R5 HIV-1 infection through their antagonistic effects on CCR5. J. Biol. Chem. 276 (37), 35194–35200.

Margolick, J.B., Munoz, A., Donnenberg, A.D., Park, L.P., Galai, N., Giorgi, J.V., O'Gorman, M.R., Ferbas, J., 1995. Failure of T-cell homeostasis preceding AIDS in HIV-1 infection. The Multicenter AIDS Cohort Study. Nat. Med. 1 (7), 674–680.

Mezzaroma, I., Carlesimo, M., Pinter, E., Alario, C., Sacco, G., Muratori, D.S., Bernardi, M.L., Paganelli, R., Aiuti, F., 1999. Long-term evaluation of T-cell subsets and T-cell function after HAART in advanced stage HIV-1 disease. AIDS 13 (10), 1187–1193.

Nath, B.M., Schumann, K.E., Boyer, J.D., 2000. The chimpanzee and other non-human-primate models in HIV-1 vaccine research. Trends Microbiol. 8 (9), 426–431.

Nathanson, N., Hirsch, V.M., Mathieson, B.J., 1999. The role of nonhuman primates in the development of an AIDS vaccine. AIDS 13 (Suppl. A), S113–S120.

O'Doherty, U., Swiggard, W.J., Jeyakumar, D., McGain, D., Malim, M.H., 2002. A sensitive, quantitative assay for human immunodeficiency virus type 1 integration. J. Virol. 76 (21), 10942–10950.

Ogg, G.S., Jin, X., Bonhoeffer, S., Moss, P., Nowak, M.A., Monard, S., Segal, J.P., Cao, Y., Rowland-Jones, S.L., Hurley, A., Markowitz, M., Ho, D.D., McMichael, A.J., Nixon, D.F., 1999. Decay kinetics of human immunodeficiency virus-specific effector cytotoxic T lymphocytes after combination antiretroviral therapy. J. Virol. 73 (1), 797–800.

Pakker, N.G., Notermans, D.W., de Boer, R.J., Roos, M.T., de Wolf, F., Hill, A., Leonard, J.M., Danner, S.A., Miedema, F., Schellekens, P.T., 1998. Biphasic kinetics of peripheral blood T cells after triple combination therapy in HIV-1 infection: a composite of redistribution and proliferation. Nat. Med. 4 (2), 208–214.

Reimann, K.A., Li, J.T., Veazey, R., Halloran, M., Park, I.W., Karlsson, G.B., Sodroski, J., Letvin, N.L., 1996a. A chimeric simian/human immunodeficiency virus expressing a primary patient human immunodeficiency virus type 1 isolate env causes an AIDS- like disease after in vivo passage in rhesus monkeys. J. Virol. 70 (10), 6922–6928.

Reimann, K.A., Li, J.T., Voss, G., Lekutis, C., Tenner-Racz, K., Racz, P., Lin, W., Montefiori, D.C., Lee-Parritz, D.E., Lu, Y., Collman, R.G., Sodroski, J., Letvin, N.L., 1996b. An env gene derived from a primary human immunodeficiency virus type 1 isolate confers high in vivo replicative capacity to a chimeric simian/human immunodeficiency virus in rhesus monkeys. J. Virol. 70 (5), 3198–3206.

Sachsenberg, N., Perelson, A.S., Yerly, S., Schockmel, G.A., Leduc, D., Hirschel, B., Perrin, L., 1998. Turnover of $CD4^+$ and $CD8^+$ T lymphocytes in HIV-1 infection as measured by Ki-67 antigen. J. Exp. Med. 187 (8), 1295–1303.

Sodora, D.L., Milush, J.M., Ware, F., Wozniakowski, A., Montgomery, L., McClure, H.M., Lackner, A.A., Marthas, M., Hirsch, V., Johnson, R.P., Douek, D.C., Koup, R.A., 2002. Decreased levels of recent thymic emigrants in peripheral blood of simian immunodeficiency virus-infected macaques correlate with alterations within the thymus. J. Virol. 76 (19), 9981–9990.

Tang, Y., Villinger, F., Staprans, S.I., Amara, R.R., Smith, J.M., Herndon, J.G., Robinson, H.L., 2002. Slowly declining levels of viral RNA and DNA in DNA/recombinant modified vaccinia virus Ankara-vaccinated macaques with controlled simian-human immunodeficiency virus SHIV-89.6P challenges. J. Virol. 76 (20), 10147–10154.

Thiebot, H., Louache, F., Vaslin, B., de Revel, T., Neildez, O., Larghero, J., Vainchenker, W., Dormont, D., Le Grand, R., 2001. Early and persistent bone marrow hematopoiesis defect in simian/human immunodeficiency virus-infected macaques despite efficient reduction of viremia by highly active antiretroviral therapy during primary infection. J. Virol. 75 (23), 11594–11602.

Ui, M., Kuwata, T., Igarashi, T., Ibuki, K., Miyazaki, Y., Kozyrev, I.L., Enose, Y., Shimada, T., Uesaka, H., Yamamoto, H., Miura, T., Hayami, M., 1999. Protection of macaques against a SHIV with a homologous HIV-1 Env and a pathogenic SHIV-89.6P with a heterologous Env by vaccination with multiple gene-deleted SHIVs. Virology 265 (2), 252–263.

Yoshimura, K., Kato, R., Yusa, K., Kavlick, M.F., Maroun, V., Nguyen, A., Mimoto, T., Ueno, T., Shintani, M., Falloon, J., Masur, H., Hayashi, H., Erickson, J., Mitsuya, H., 1999. JE-2147: a dipeptide protease inhibitor (PI) that potently inhibits multi-PI-resistant HIV-1. Proc. Natl. Acad. Sci. USA 96 (15), 8675–8680.

ELSEVIER

Journal of Clinical Virology 33 (2005) 188–193

JOURNAL OF CLINICAL VIROLOGY

www.elsevier.com/locate/jcv

Spontaneous recovery of hemoglobin and neutrophil levels in Japanese patients on a long-term Combivir® containing regimen

Shuzo Matsushita[a,d,*], Kazuhisa Yoshimura[a,d], Tetsuya Kimura[a], Asako Kamihira[b], Misao Takano[c], Kenichiro Eto[d], Takuma Shirasaka[b], Hiroaki Mitsuya[d], Shinichi Oka[c]

[a] *Division of Clinical Retrovirology and Infectious Diseases, Center for AIDS Research, Kumamoto University, 2-2-1 Honjo, Kumamoto 860-0811, Japan*
[b] *Department of Immunological and Infectious Diseases, Osaka National Hospital, Osaka 540-0006, Japan*
[c] *AIDS Clinical Center, International Medical Center of Japan, Tokyo 162-8655, Japan*
[d] *Department of Infectious Diseases, Kumamoto University School of Medicine, Kumamoto 860-8556, Japan*

Received 11 August 2004; accepted 3 November 2004

Abstract

Objective: In order to evaluate long-term toxicity of Combivir, we retrospectively reviewed clinical records of HIV-1 infected cases under treatment with Combivir-containing regimen and we analyzed the clinical data compared to other NRTIs-containing regimens.
Study design: A total of 55 patients who were on Combivir and 39 on a control regimen were examined.
Results: After starting treatment with Combivir-containing regimens viral load and $CD4^+$ T-cell count improved as well as the control group. Rates of adverse events in Combivir group and ZDV (400 mg/day) + 3TC group were 50.9% (28/55) and 60% (12/20), respectively. Some of these Japanese patients who started Combivir regimen as a first-line HAART (primary Combivir group) showed some decrease in hemoglobin levels or neutrophil counts within 6 months. However, a significant recovery of these indices of hematological toxicities occurred in patients who continued the regimen for 18–24 months.
Conclusion: Our findings suggest that the safety of 600 mg of ZDV is similar to 400 mg/day of ZDV and the existence of mechanisms that compensate for anemia and for the neutropenia associated with long-term use of Combivir.

Keywords: Combivir; Zidovudine; Lamivudine; Hemoglobin; Neutrophil; Long-term treatment

1. Introduction

Prognosis of HIV infections dramatically improved after introduction of highly active anti-retro viral therapy (HAART). However, the occurrence of adverse events and drug resistance during long-term use of anti-retrovirals are now big issues (Yeni et al., 2002; Dieleman et al., 2002). Present HAART also has a problem to maintain a high adherence because of the pill burden and patients' quality of life is affected. Combivir® is a fixed dose combination tablet containing zidovudine (ZDV) and lamivudine (3TC) (Eron et al., 2000). Each tablet contains 300 mg of ZDV and 150 mg of 3TC and has been widely used as a nucleoside reverse transcriptase inhibitor (NRTI) component of HAART against HIV-1 infection.

HIV infection and AIDS are known to be associated with a significant hematological toxicity, including anemia, neutropenia, and thrombocytopenia (Moses et al., 1998). In addition, studies with zidovudine have shown that this drug may compound the hematological toxicity of HIV and lead to an independent development of anemia and neutropenia (Wilde and Langtry, 1993). Consistent with these observations, the incidence of anemia or neutropenia in mildly or asymptomatic adults treated with zidovudine was between 1.1% and 9.7%, whereas in adults with AIDS or the AIDS related complex it ranged from 15% to as high as 61% (Wilde

* Corresponding author. Tel.: +81 96 373 6536; fax: +81 96 373 6537.
E-mail address: shuzo@kaiju.medic.kumamoto-u.ac.jp (S. Matsushita).

1386-6532/$ – see front matter © 2004 Elsevier B.V. All rights reserved.
doi:10.1016/j.jcv.2004.11.002

and Langtry, 1993). In Japan, many physicians prescribe low dose ZDV such as 400 mg/day to avoid drug-induced anemia and neutropenia even though the standard dose of ZDV is 500–600 mg/day in United States (Kimura et al., 1992, 1998). Given the dose-dependent nature of these adverse effects, they are concerned about increased risk of hematological toxicity using Combivir that contains 600 mg of ZDV as the daily dose for Japanese patients who have lower body weights compared to patients in United States. Moreover, long-term consequence of the hematological toxicity resulting from continuous use of Combivir has not been well defined. We retrospectively reviewed clinical records of HIV-1 infected cases under treatment of Combivir-containing regimen used in three hospitals in Japan and we analyzed clinical data cross-sectionally to evaluate long-term toxicity of Combivir.

2. Patients and methods

HIV-1 positive Japanese patients were recruited from Kumamoto University Hospital, Osaka National Hospital and International Medical Center of Japan from June 1999 (after the Combivir launch) until June 2003. The clinical record was investigated in a retrospective manner. All collected cases were separated into four groups, as follows;

Primary Combivir Group (PCV): started Combivir as a first-line HAART.
Secondary Combivir Group (SCV): changed to Combivir from other NRTIs.
Primary Control Group (PCO): started NRTIs (except for Combivir) as a first-line HAART.
Secondary Control Group (SCO): changed to NRTIs except Combivir from other NRTIs.

We checked hemoglobin levels and neutrophil counts to examine the influence on hematological toxicity of ZDV every 6 months. We analyzed the data that could be followed over 18 months for removing various biases such as drop out cases with abnormal laboratory test values. Moreover, we also checked the HIV-RNA, $CD4^+$ T-cell counts and other laboratory test data every 6 months. We also checked any adverse events. This study was done under the approval of the Institutional Review Board of the Kumamoto University Hospital, Japan. All participants provided written informed consent.

3. Results

3.1. Patients' characteristics

Of the 94 data on subjects were 55 who were on Combivir (PCV: 27, SCV: 28) and 39 were on control regimens (PCO: 29, SCO: 10). The NRTIs used in the control group included of 20 cases of ZDV (400 mg/day) + 3TC, 18 cases of stavudine (d4T) + 3TC and one case of d4T + didanosine (ddI). Patients' characteristics are shown in Table 1. A couple of factors are statistically different such as the sex ($p < 0.01$: Fisher's exact test), weight ($p < 0.05$: Student's t-test) and Karnofsky score ($p = 0.0062$: Student's t-test) between Combivir group and control group. Combivir was likely to be used for patients with a higher baseline weight and the males. The mean viral load at baseline in Combivir group was $10^{3.9}$ copies/mL and for the control group was $10^{4.1}$ copies/mL. There was no statistical difference between the groups. The baseline $CD4^+$ T-cell counts in Combivir group were higher than in the control group significantly ($393/mm^3$ versus $263/mm^3$; $p = 0.0101$: Student's t-test). Most patients were prescribed efavirenz (EFV) or nelfinavir (NFV) as a concomitant drug. Fifty-two percent of all patients were on EFV and 16% were taking NFV. The Combivir group had more combination cases with EFV than did the control group, because these two drugs approved for use in Japan at the same period have similar characteristics such as small pill counts and frequency of ingestion.

3.2. Effects on hemoglobin levels

To avoid biases in the data resulting from inclusion of patients with a shorter time follow up, including drop out cases, we focused on the patients that could be followed for over 18 months. Mean hemoglobin levels at baseline of Combivir group (PCV group: 13.9 g/dL, SCV group: 14.2 g/dL) were higher than for the control group (PCO group: 13.1 g/dL, SCO group: 13.7 g/dL) (Fig. 1A). It seems Combivir was likely to give to those with a lesser risk of anemia. We divided patients in PCV group into two sub-groups such as hemoglobin level decreased (sub-group A; $n = 10$) and not changed or increased (sub-group B: $n = 8$) at 6 months after starting Combivir. Fig. 1B shows a trend of hemoglobin levels in sub-group A. Each hemoglobin level at 6, 12, 18 and 24 months after starting treatment decreased significantly compared to baseline ($p < 0.005$, $p < 0.005$, $p < 0.005$ and $p < 0.05$, respectively; Wilcoxon matched pairs signed rank test). However, the decreased hemoglobin levels at 6 months gradually recovered to the baseline level despite continuation of the same regimen. The hemoglobin level at 18, 24 months increased significantly compared to 6-month values ($p < 0.05$ and $p < 0.005$, respectively). On the other hand, the hemoglobin level of sub-group B did not decrease for 18–30 months of follow up period (data not shown). The difference of background between sub-groups A and B was baseline level of hemoglobin and hematocrit. These levels in sub-group A were higher than for sub-group B statistically (14.9 ± 1.2 versus 12.6 ± 0.7; $p < 0.001$, 44.4 ± 3.2 versus 37.4 ± 2.0; $p < 0.001$, Student's t-test).

3.3. Effects on neutrophil counts

The trend of mean neutrophil counts was similar to counts for hemoglobin levels. Mean neutrophil counts of all groups

Table 1
Baseline characteristics

	Combivir group (PCV + SCV) ($n = 55$)	Control group (PCO + SCO) ($n = 39$)	p-value
Sex (male/female)	54/1	32/7	0.00815[a]
Age	35.9 ± 9.5 (22–68)	38.6 ± 10.7 (23–78)	0.2117[b]
Weight (kg)	64.6 ± 10.8 (47.0–91.6)	59.6 ± 11.2 (36.4–81.0)	0.0303[b]
Hemophilia			
Non	48	32	0.562[a]
A	5	7	
B	2	0	
Baseline VL (log)			
<2.6	19	11	0.4432[b]
2.6–3	1	1	
3–4	6	4	
4–5	11	13	
>5	15	10	
Unknown	3	0	
Mean ± S.D.	3.9 ± 1.2	4.1 ± 1.2	
Range	2.6–5.9	2.6–5.9	
Baseline CD4 count			
<200	14	14	0.0101[b]
200–500	25	19	
>500	13	5	
Unknown	3	1	
Mean ± S.D.	393 ± 265	263 ± 179	
Range	1–1132	5–607	
CDC class			
A1	5	3	0.8064[c]
A2	22	17	
A3	6	13	
B1	2	0	
B2	3	0	
B3	2	5	
C1	3	0	
C3	12	11	
Karnofsky score			
20%	0	1	0.0062[b]
40%	0	2	
50%	0	1	
60%	1	0	
70%	0	1	
80%	4	6	
90%	11	8	
100%	39	20	
Mean ± S.D.	95.8 ± 7.9	87.7 ± 19.4	

[a] Fisher' exact test.
[b] Student's t-test.
[c] Wilcoxon 2-sample test.

were over 2000/mm^3 and did not have statistically change from the baseline during the follow up period (Fig. 1C). We separated subjects in the PCV group into two sub-groups as well as for hemoglobin levels to examine the toxicity of Combivir to neutrophils. In the sub-group C ($n = 10$) those with mean neutrophil counts decreased and the sub-group D ($n = 7$) included subjects with no changes or increased neutrophil counts at 6 months after being on Combivir. Fig. 1D shows the trend of the neutrophil counts in sub-group C. Neutrophil counts at 6, 12, 18 and 24 months after starting the treatment decreased significantly compared to baseline ($p < 0.005$, $p < 0.05$, $p < 0.05$ and $p < 0.05$, respectively; Wilcoxon matched pairs signed rank test). However, the decreased neutrophil counts gradually recovered as did hemoglobin levels. The mean neutrophil counts at 18 months increased significantly compared to data at 6 months ($p < 0.05$; Wilcoxon matched pairs signed rank test).

3.4. Effects on other laboratory test value

MCV values at baseline for the secondary treatment group such as SCV group and SCO group were higher than for pri-

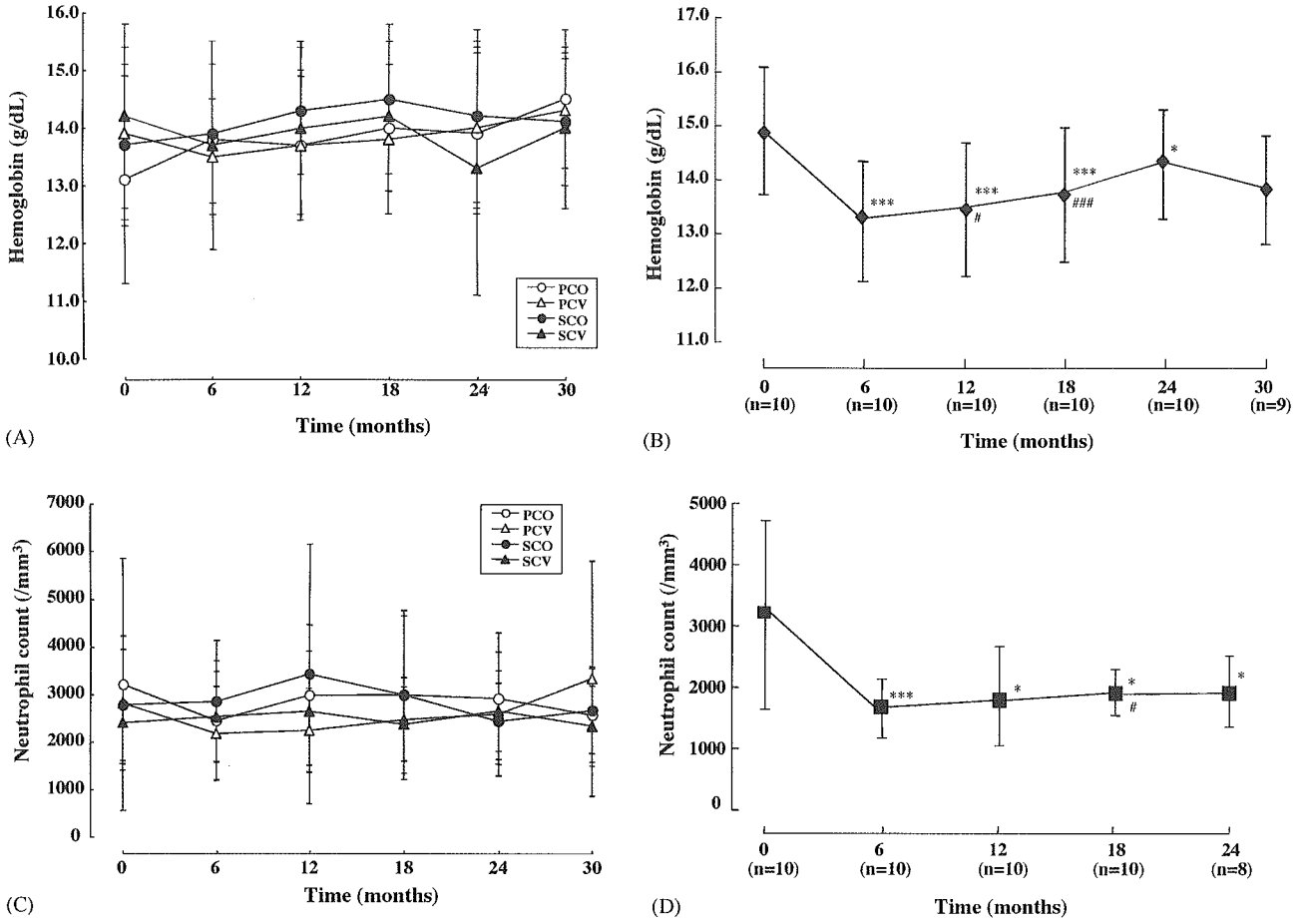

Fig. 1. Recovery after transient suppression of hemoglobin and neutrophil levels in patients with long-term use of Combivir. (A) Mean hemoglobin levels did not change significantly in all groups during each treatment. The baseline hemoglobin level in the Combivir group (PCV + SCV) was higher than in controls (PCO + SCO). (B) Mean hemoglobin levels at 6, 12, 18 and 24 months after start of treatment decreased significantly compared to baseline in the subgroup A of PCV group ($n = 10$). However the decreased hemoglobin level gradually reverted to the baseline levels despite continuation of the same regimen. Hemoglobin levels at 12 and 18 months were significantly high compared to findings at 6 months. (Wilcoxon matched pairs signed rank test; $^{*,\#}p < 0.05$, $^{***,\#\#\#}p < 0.005$). (C) Mean neutrophil counts did not change significantly in all groups during each treatment. (D) Mean neutrophil counts at 6, 12, 18 and 24 months after beginning treatment decreased significantly compared to baseline in sub-group C of PCV group ($n = 10$). However, the neutrophil counts gradually reverted to baseline levels despite continuation of the same regimen. The neutrophil counts at 18 months was significantly high compared to that of 6 months (Wilcoxon matched pairs signed rank test; $^{*,\#}p < 0.05$, $^{***}p < 0.005$).

mary treatment groups such as PCV group and PCO group. It seems ZDV or d4T in the secondary treatment group affected red blood cell counts. However, after starting each treatment, MCV values increased and became high at around 110/mm^3 in all groups (Fig. 2A). Other laboratory test values did showed no notable changes (data not shown).

3.5. Adverse events

The most common adverse events in each group were nausea/vomiting, dizziness and malaise. Anemia was observed in two in the Combivir group and one in the control group. Discontinuing each treatment led to elimination of these adverse effects. The anemia in two in the Combivir group was observed 2 months after their starting treatment, and that in one in the control group was evident as early as the eighth day. The occurrence of anemia in the control group was on ZDV 400 mg/day + 3TC. The frequency of anemia in the Combivir group was 3.6% (2/55) and similar to that in the control group {2.6% (1/39)}. The 20 in the control group on ZDV + 3TC regimen were on a ZDV 400 mg/day. We compared the safety profile of ZDV 600 mg/day to ZDV 400 mg/day. Adverse events rate of Combivir was 50.9% (28/55) and 60.0% (12/20) of AZT + 3TC group. Moreover, the number who discontinued Combivir group was 7 (12.7%) and that in ZDV + 3TC group was 5 (25.0%). In the SCV group, nineteen were changed to Combivir from ZDV 400 mg/day + 3TC. There were six with some adverse events and these were similar to other groups' events. These observations suggest that increasing the ZDV dose to 600 mg/day does not affect the incidence of adverse events. In addition there were no concomitantly used drugs that could affect pharmacokinetic parameters of ZDV and enhance its toxicity.

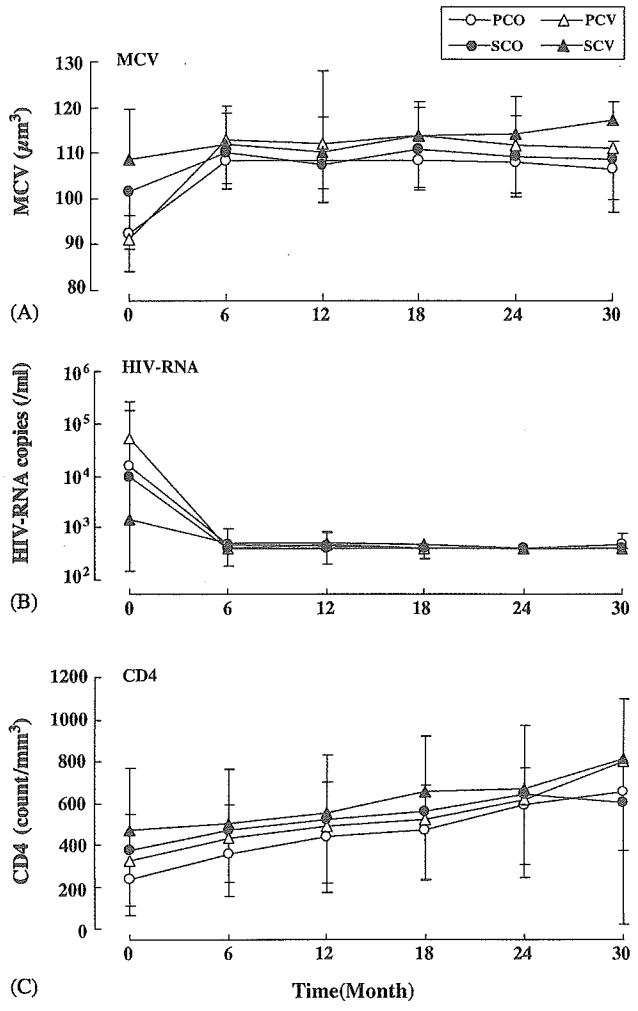

Fig. 2. Changes in MCV values, HIV RNA level and CD4$^+$ T cell counts in each group of patients. (A) MCV values for the secondary treatment group such as SCV and SCO group were higher than for primary treatment groups such as PCV and PCO group at baseline. However, after starting each treatment, MCV values increased and became high at around 110/mm^3 in all groups. (B) Mean HIV RNA level in all groups of treatment decreased compared to baseline significantly ($p < 0.05$–$p < 0.001$; Wilcoxon matched pairs signed rank test). (C) Mean CD4$^+$ T cell counts in all groups of treatment increased significantly compared to the baseline ($p < 0.05$–$p < 0.001$; Wilcoxon matched pairs signed rank test).

3.6. Effects on viral load and CD4$^+$ T-cell counts

Baseline viral load in the primary treatment group (PCV + PCO) was higher than in the secondary treatment group (SCV + SCO). Mean baseline viral loads of each group were $10^{4.6}$ copies/mL (PCV), $10^{4.0}$ copies/mL (PCO), $10^{3.0}$ copies/mL (SCV) and $10^{3.7}$ copies/mL (SCO), respectively. However, after starting each treatment, HIV RNA was not detectable in serum samples from in each group (VL < 50 or <400 copies/mL) (Fig. 2B). Baseline CD4$^+$ T-cell count in the SCV group was 518/mm^3 and higher than other groups (PCV: 304/mm^3, SCO: 345/mm^3, PCO: 277/mm^3) significantly ($p < 0.001$; Student's t-test) (Fig. 2C). This result suggests effective treatment with the previous combination for the SCV group. CD4$^+$ T-cell counts during each treatment increased significantly ($p < 0.05$–$p < 0.001$; Wilcoxon matched pairs signed rank test) and reached over 600/mm^3 at 30 months in all groups (Fig. 2C).

4. Discussion

The nucleoside reverse transcriptase inhibitor (NRTI) was first developed as an anti-HIV drug. However, the appropriate dosage was unclear because this type of drug is only active after being phosphorylated inside cells. A daily dose of 400 mg of ZDV has been widely used in Japan because anemia and neutropenia occurred frequently in cases of ingesting a higher dose (800 mg/day) than did 400 mg/day of ZDV in a clinical trial conducted in Japan (Kimura et al., 1992). Bone marrow toxicity associated with AZT such as macrocytic anemia and neutropenia has been frequently reported for the patients treated with a higher dose of ZDV mono therapy (Richman et al., 1987). Given the dose-dependent nature of these adverse effects, Japanese health care providers have some hesitance to prescribe Combivir that contains 600 mg of ZDV, as the daily dose. Data on four patients with severe anemia associated with Combivir have also been reported (Sibery et al., 2003). To evaluate the long-term toxicity of Combivir, we reviewed clinical records of HIV-1 infected Japanese patients on treatment with Combivir-containing regimen.

The results in this retrospective study showed that anemia and adverse events occurred at comparable frequency in each group of patients. Consistent with previous reports (Hester and Peacock, 1998; Tseng et al., 1998) these adverse events occurred in less than a few months after starting each treatment. The frequency of anemia in the Combivir group was only 3.7% (2/54), and it was similar to that for ZDV 400 mg/day + 3TC group (5.0%) group. In other words there was no difference in these groups with respect to the frequency of anemia by the difference in the dose of ZDV. It is also of note that the efficacy of Combivir was comparable to that of 400 mg of ZDV of four times a day with a twice a day dosing of 3TC. However, we have to take into account the fact that Combivir was prescribed for heavy weight patients. And such may mask the occurrence of adverse events as well as the difference in efficacy.

We observed a certain degree of decrease in hemoglobin levels and neutrophil counts in the subgroups of patients in PCV (subgroups A and C, respectively). Interestingly, a gradual recovery of these hematological toxicities occurred despite the continuation of Combivir containing regimens. The mechanism whereby the risk of hematological toxicity associated with increasing ZDV dosages may be related to the intracellular accumulation of the toxic metabolite zidovudine monophosphate (AZTMP) (Tornevik et al., 1995). AZTMP interferes with both cellular DNA synthesis and exonuclease-catalyzed removal of ZDV from host cell DNA (Sommadossi et al., 1989; Harrington et al., 1993). In addition, at clinically

relevant concentrations, AZTMP acts as a potent inhibitor of the transport of pyrimidine nucleotide sugars into the Golgi complex, thereby inhibiting protein glycosylation and altering glycosphingolipid synthesis (Yan et al., 1995). Therefore, AZTMP may elicit cytotoxic effects on rapidly growing erythrocytes and neutrophil precursors, both by interfering with nuclear DNA replication and by compromising the function of membrane receptors involved in receiving of extracellular stimuli required for cell growth and differentiation. From these observations it seems reasonable to speculate that either decrease in the intracellular concentration of AZTMP or compensatory mechanisms that improve the signal transduction for erythropoiesis and myelopoiesis mediated by cytokines contributed the recovery from hematological toxicities.

Two mechanisms may be related to the decrease in the concentration of AZTMP: altered metabolism of nucleoside analogues due to impaired nucleoside phosphorylation and increased efflux of the compounds by membrane transport mechanisms (Schuetz et al., 1999; Wijnholds et al., 2000). These mechanisms have been considered to contribute to the cellular drug-resistance (Dianzani et al., 1994; Groschel et al., 1997; Fridland et al., 2000; Turriziani et al., 2000). However, there was no evidence of treatment failure for patients in our PCV group as we found an increase in $CD4^+$ cell counts and ah undetectable HIV-RNA load. Furthermore, the MCV level which is associated with the intracellular increase of AZTMP was kept high. These observations suggest that decrease in the level of AZTMP in the course of long-term treatment is unlikely although we must determine longitudinal changes of intracellular AZTMP level in precursors of blood cells in patients on Combivir treatment. Other compensatory mechanisms against the hematological toxicity may occur. An increase in erythropoietin or granulocyte-colony stimulating factor (G-CSF) levels in compensation for chronic anemia or neutropenia is another notion.

Acknowledgments

This work was supported in part by the Ministry of Health, Labor and Welfare of Japan (H-15-AIDS-001, -011, -015 and H-13-AIDS-001).

References

Dianzani F, Antonelli G, Turriziani O, Riva E, Simeoni E, Signoretti C, et al. Zidovudine induces the expression of cellular resistance affecting its antiviral activities. AIDS Res Hum Retroviruses 1994;10:1471–8.

Dieleman JP, Jambroes M, Gyssens IC, Sturkenboom MC, Stricker BH, Mulder WM, et al. Determinants of recurrent toxicity-driven switches of highly active antiretroviral therapy. The ATHENA Cohort. AIDS 2002;16:737–45.

Eron JJ, Yetzer ES, Ruane PJ, Becker S, Sawyerr GA, Fisher RL, et al. Efficacy, safety, and adherence with a twice-daily combination of lamivudine/zidovudine tablet formulation, plus a protease inhibitor, in HIV infection. AIDS 2000;14:671–81.

Fridland A, Connelly MC, Robbins BL. Cellular factors for resistance against antiretroviral agents. Antiviral Ther 2000;5:181–5.

Groschel B, Cinatl J, Cinatl Jr J. Viral and cellular factors for resistance against antiretroviral agents. Intervirology 1997;14:400–7.

Harrington JA, Reardon JE, Spector T. 3′-Azido-3′-deoxythymidine (AZT) monophosphate: an inhibitor of exonucleolytic repair of AZT terminated DNA. Antimicrob Agents Chemother 1993;37: 918–20.

Hester EK, Peacock Jr JE. Profound and unanticipated anemia with lamivudine-zidovudine combination therapy in zidovudine-experienced patients with HIV infection. AIDS 1998;12:439–40.

Kimura S, Oka S, Toyoshima T, Hirabayashi Y, Kikuchi Y, Mitamura K, et al. A randomized trial of reduced doses of azidothymidine in Japanese patients with human immunodefiency virus type 1 infection. Intern Med 1992;31:871–6.

Kimura S, Yamada K, Ito A, Mimaya J, Takamatsu J, 3TC Study Group. Phase 2 clinical study on 3TC (Lamivudine) in HIV infections. Antibiot Chemother 1998;14:1419–32.

Moses A, Nelson J, Bagby Jr GC. Review article: the influence of human immunodeficiency virus-1 on hematopoiesis. Blood 1998;91:1479–95.

Richman DD, Fischl MA, Grieco MH, Gottlieb MS, Volberding PA, Laskin OL, et al. The toxicity of azidothymidine (AZT) in the treatment of patients with AIDS and AIDS-related complex. A double-blind, placebo-controlled trial. N Engl J Med 1987;317:192–7.

Schuetz JD, Connelly MC, Sun D, Paibir SG, Flynn PM, Srinivas RV, et al. MRP4: a previously unidentified factor in resistance to nucleoside-based antiviral drugs. Nat Med 1999;5:1048–51.

Sibery MJ, Astrow A, Kempin S, Halperin I. Combivir (AZT/3TC) therapy is associated with life-threatening anemia in patients with HIV infection. Blood 2003;102:51b (Abstract 3907).

Sommadossi JP, Carlisle R, Zhou Z. Cellular pharmacology of 3-azido-3′-deoxythymidine with evidence of incorporation into DNA of human bone marrow cells. Mol Pharmacol 1989;36:9–14.

Tornevik Y, Ullman B, Balzarini J, Wahren B, Eriksson S. Cytotoxicity of 3′-azido-3′-deoxythymidine correlates with 3′-azidothymidine-5′-monophosphate (AZTMP) levels, whereas anti-human immunodeficiency virus (HIV) activity correlates with 3′-azidothymidine-5′-triphosphate (AZTTP) levels in cultured CEM T-lymphoblastoid cells. Biochem Pharmacol 1995;49:829–37.

Tseng A, Conly J, Fletcher D, Keystone D, Salit I, Walmsley S. Precipitous declines in hemoglobin levels associated with combination zidovudine and lamivudine therapy. Clin Infect Dis 1998;27:908–9.

Turriziani O, Antonelli G, Dianzani F. Cellular factors involved in the induction of resistance of HIV to antiretroviral agents. Int J Antimicrob Agents 2000;16:353–6.

Wijnholds J, Mol CA, van Deemter L, de Haas M, Scheper GL, Baas F, et al. Multidrug-resistance protein 5 is a multispecific organic anion transporter able to transport nucleotide analogs. Proc Natl Acad Sci USA 2000;97:7476–81.

Wilde MI, Langtry HD. Zidovudine. An update of its pharmacodynamic and pharmacokinetic properties, and therapeutic efficacy. Drugs 1993;46:515–78.

Yan JP, Ilsley DD, Frohlick C, et al. 3′-Azidothymidin (zidovudine) inhibits glycosylation and dramatically alters glycosphingolipid synthesis in whole cells at clinically relevant concentrations. J Biol Chem 1995;270:22836–41.

Yeni PG, Hammer SM, Carpenter CCJ, Cooper DA, Fischl MA, Gatell JM, et al. Antiretroviral treatment for adult HIV infection. 2002. Updated recommendation of the International AIDS Society-USA Panel. JAMA 2002;288:222–35.

Generation of High-Affinity Antibody against T Cell-Dependent Antigen in the *Ganp* Gene-Transgenic Mouse[1]

Nobuo Sakaguchi,[2]*¶ Tetsuya Kimura,† Shuzo Matsushita,† Satoru Fujimura,* Junji Shibata,† Masatake Araki,‡ Tamami Sakamoto,§ Chiemi Minoda,§ and Kazuhiko Kuwahara*‖

Generation of high-affinity Ab is impaired in mice lacking germinal center-associated DNA primase (GANP) in B cells. In this study, we examined the effect of its overexpression in *ganp* transgenic C57BL/6 mice ($Ganp^{Tg}$). $Ganp^{Tg}$ displayed normal phenotype in B cell development, serum Ig levels, and responses against T cell-independent Ag; however, it generated the Ab with much higher affinity against nitrophenyl-chicken gammaglobulin in comparison with C57BL/6. To further examine the affinity increase, we established hybridomas producing high-affinity mAbs and compared their affinities using BIAcore. C57BL/6 generated high-affinity anti-nitrophenyl mAbs ($K_D \sim 2.50 \times 10^{-7}$ M) of IgG1/λ1 and contained the $V_H186.2$ region with W33L mutation. $Ganp^{Tg}$ generated much higher affinity ($K_D > 1.57 \times 10^{-9}$ M) by usage of $V_H186.2$ as well as noncanonical V_H7183 regions. $Ganp^{Tg}$ also generated exceptionally high-affinity anti-HIV-1 (V3 peptide) mAbs ($K_D > 9.90 \times 10^{-11}$ M) with neutralizing activity. These results demonstrated that GANP is involved in *V* region alteration generating high-affinity Ab. *The Journal of Immunology,* 2005, 174: 4485–4494.

The Ag-driven B cells expressing high-affinity BCR, which have been selected in secondary lymphoid organs, generate high-affinity Ab. Ag-driven B cells proliferate rapidly by the stimulation with Ag and costimulatory molecules from Th cells surrounding the germinal center (GC)[3] region, in which such B cells undergo affinity maturation of Ig V region and class switching of the C region during the response to T cell-dependent Ag (TD-Ag) in vivo (1, 2). For affinity maturation, introduction of somatic hypermutation (SHM) in the *V* region is probably essential and, in addition to this molecular alteration, the Ag-driven B cells with high-affinity BCR must be selected or further enriched during the maturation of Ag-driven B cells in GCs.

A 210-kDa germinal center-associated DNA primase (GANP) protein, bearing RNA-primase and minichromosome maintenance (MCM)3-binding activities, is up-regulated in GC B cells upon immunization with TD-Ag in vivo and is induced by the stimulation to BCR and CD40 in vitro (3, 4). The mutant mouse with *ganp* gene knockout B cells (B-$ganp^{-/-}$) has a severe defect in mounting high-affinity Ab responses to TD-Ag (5), suggesting that GANP is required for generation of high-affinity Ab in response to TD-Ag in vivo. However, there remained several possibilities to account for the molecular mechanism in generation of high-affinity V regions by the expression of GANP in GC B cells. GANP might augment the induction of SHM in the *V* regions, resulting in the affinity maturation of V regions during the proliferation and differentiation of Ag-driven B cells in GCs. Alternatively, GANP might be involved in the survival of the high-affinity BCR^+ B cells for the positive selection through the interaction of Ags captured on the follicular dendritic cell network. The GCs of the B-$ganp^{-/-}$ mice displayed an increase of apoptotic cells upon immunization with TD-Ag SRBC, which suggested a partial involvement of GANP in the survival of GC B cells. However, the $ganp^{-/-}$ B cells do not show marked abnormalities in the levels of apoptotic and proapoptotic molecules after BCR cross-linkage (5). To study the function of GANP in generation of high-affinity Ab response, it is necessary to examine whether the affinity maturation of BCR on the GC B cell is generated by the genetic alteration in the *V* region gene.

We speculated that it would be possible to generate a high-affinity Ab if we used mice with higher level GANP expression in B cells. We studied whether the transgenic mouse with increased expression of *ganp* gene could generate high-affinity Ab against TD-Ag using a model epitope of 4-hydroxy-3-nitrophenyl acetyl (NP)-hapten in the C57BL/6 background. To demonstrate the increased affinity of the Ab in detail, we established the hybridomas secreting anti-NP mAbs after immunization with NP-chicken gammaglobulin (CG) in $Ganp^{Tg}$ mice. After selecting the high-affinity mAbs against NP-hapten by differential ELISA method and the BIAcore system, we examined the *V* region gene usage of the hybridomas and compared the sequences with those from wild-type C57BL/6 mice. The results suggest that the affinity maturation of BCR on GC B cells is generated by the altered V_H region usage with increased SHM in $Ganp^{Tg}$ mice.

Materials and Methods

$Ganp^{Tg}$ *mouse*

The expression construct of mouse *ganp* cDNA under the mouse Ig promoter and human Ig enhancer (6) was used for establishing the transgenic

*Department of Immunology, Graduate School of Medical Sciences, †Division of Clinical Retrovirology and Infectious Diseases, Center for AIDS Research, ‡Division of Bioinformatics, Institute of Resource Development and Analysis, Kumamoto University, and §Trans Genic, Kumamoto Japan; ¶Core Research for Evolutional Science and Technology Program, Saitama Japan; and ‖PRESTO, Japan Science and Technology Agency, Saitama, Japan

Received for publication October 26, 2004. Accepted for publication January 4, 2005.

The costs of publication of this article were defrayed in part by the payment of page charges. This article must therefore be hereby marked *advertisement* in accordance with 18 U.S.C. Section 1734 solely to indicate this fact.

[1] This work was supported by Special Coordination Funds for Promoting Science and Technology from the Ministry of Education, Culture, Sports, Science and Technology of Japan, Matching Funds from New Energy and Industrial Technology Development Organization, and grants from the Core Research for Evolutional Science and Technology Program, Japan Science and Technology Agency.

[2] Address correspondence and reprint requests to Dr. Nobuo Sakaguchi, Department of Immunology, Graduate School of Medical Sciences, Kumamoto University, 1-1-1, Honjo, Kumamoto 860-8556, Japan. E-mail address: nobusaka@kaiju.medic.kumamoto-u.ac.jp

[3] Abbreviations used in this paper: GC, germinal center; GANP, germinal center-associated DNA primase; NP, 4-hydroxy-3-nitrophenyl acetyl; SHM, somatic hypermutation; TD-Ag, T cell-dependent Ag; MCM, minichromosome maintenance; CG, chicken gammaglobulin; KLH, keyhole limpet hemocyanin; TNP, 2,4,6-trinitrophenyl; LTR, long terminal repeat.

0022-1767/05/$02.00

mouse by the standard procedure. Mice were screened for the transgene by PCR using *ganp* 1–5′ primer (5′-TCCCGCCTTCCAGCTGTGAC-3′) and *ganp* 1–3′ primer (5′-GTGCTGCTGTGTTAT GTCCT-3′) and Southern blot analysis using *ganp* probe A (1143–2193 nt) of tail genomic DNAs. The *Ganp*^{Tg} mice that express 1.5- to 2.0-fold increase of *ganp* gene grew normally under specific pathogen-free condition and were immunized with Ags. *Ganp* transcripts were detected by two primers (*ganp* 1–5′ and *ganp* 1–3′) in comparison with *β-actin* control (5). All mice were maintained in the Center for Animal Resources and Development (Kumamoto University, Kumamoto, Japan).

Flow cytometric analysis

Single-cell suspensions from lymphoid organs were stained with each biotin-labeled mAb in combination with FITC-conjugated streptavidin (Amersham Biosciences) and PE-conjugated mAbs. Lymphoid cells were analyzed by FACSCalibur (BD Biosciences) using CellQuest software.

In vitro proliferation assay

Purified B cells were cultured for 48 h at a density of 2×10^5 cells/well in 96-well microtiter plates in RPMI 1640 medium containing 10% heat-inactivated FCS (JRH Biosciences), 2 mM L-glutamine, and 5×10^{-5} M 2-ME. The cells stimulated with or without various mitogenic stimulants were pulsed with 0.2 μCi/well of [^{3}H]thymidine (ICN Pharmaceuticals) for 16 h before harvesting, and the incorporated radioactivity was measured by scintillation counter. Stimulatory reagents were affinity-purified goat anti-mouse μ-chain-specific Ab ($F(ab')_2$, 10 μg/ml; ICN Pharmaceuticals), rat anti-mouse CD40 mAb (LB429, 10 μg/ml) (4), and LPS (10 μg/ml; Sigma-Aldrich).

Immunohistochemistry

The 8-μm sections of spleen from SRBC-immunized mice were lightly fixed with acetone. Slides were blocked with 3% BSA in PBS-Tween 20

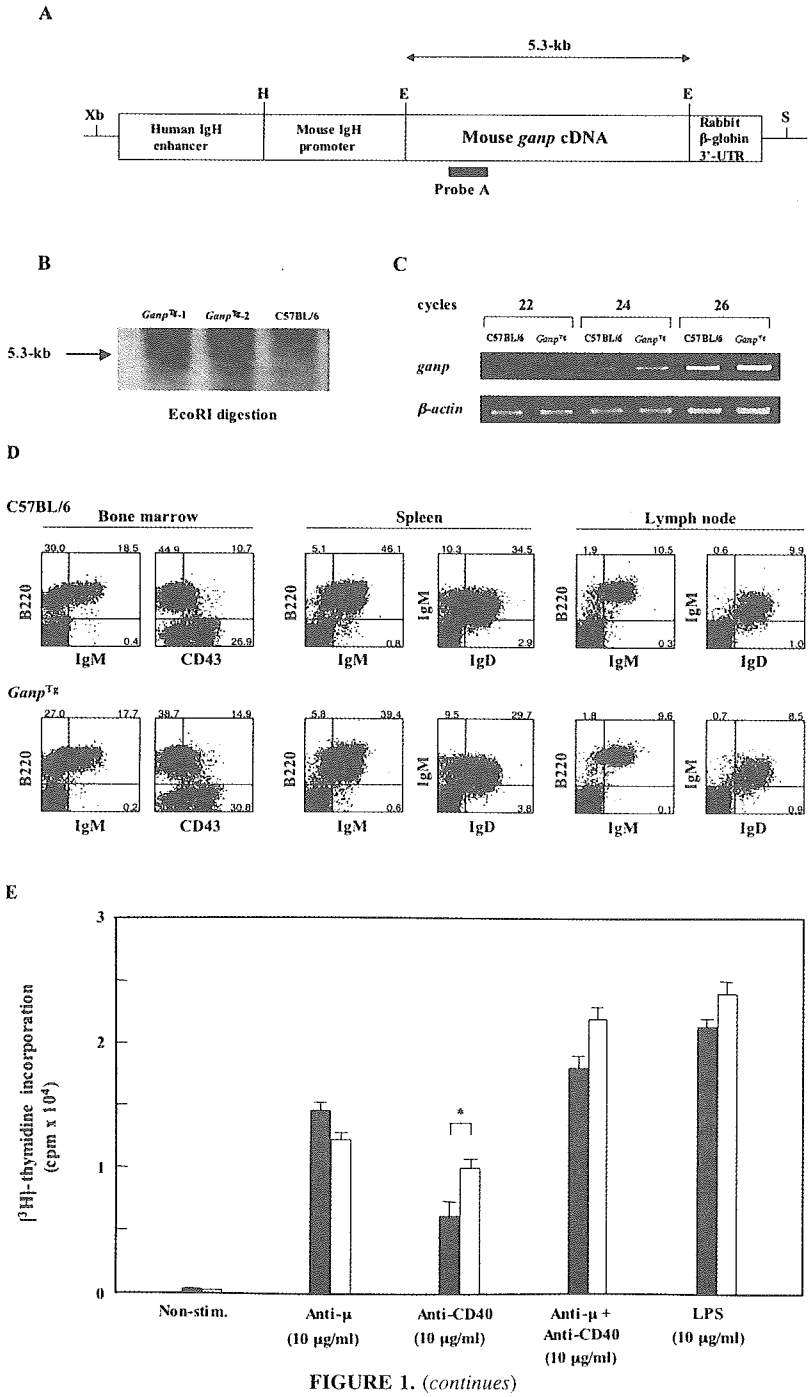

FIGURE 1. Generation of transgenic mice that overexpress the *ganp* gene in B cells. *A*, A schematic diagram of construct for *Ganp*^{Tg} under the human Ig enhancer, mouse Ig promoter, and followed by rabbit β-globin 3′-untranslated region (UTR). The construct contains restriction enzyme sites: Xb, *Xba*I; H, *Hin*dIII; E, *Eco*RI; and S, *Sal*I. The probe for Southern blot analysis (probe A) is indicated. *B*, Detection of the *ganp* transgene by Southern blot analysis. Southern blot analysis with *Eco*RI-digested genomic DNAs of *Ganp*^{Tg} displayed a 5.3-kb band hybridized with probe A. *C*, Up-regulation of *ganp* transcripts in B cells from *Ganp*^{Tg}. Semiquantitative PCR was performed using the primers *ganp* 1–5′ and *ganp* 1–3′, in comparison with *β-actin* transcripts. From densitometer analysis, *ganp* transcripts in B cells from *Ganp*^{Tg} showed an 80% increase in comparison with C57BL/6 mice. *D*, Flow cytometric analysis. Bone marrow, spleen, and lymph node cells from 8-wk-old C57BL/6 and *Ganp*^{Tg} were analyzed with indicated markers. *E*, In vitro proliferation assay of purified B cells from *Ganp*^{Tg}. [^{3}H]Thymidine incorporation was measured in the presence or absence of B cell mitogenic stimulants in C57BL/6 mice (■) and *Ganp*^{Tg} mice (□). The representative data are shown from four independent experiments. *, $p < 0.05$. *F*, Kinetics of GC formation after TD-Ag in *Ganp*^{Tg}. C57BL/6 and *Ganp*^{Tg} mice were immunized by SRBC. At day 10 or day 14, the sections were doubly immunostained with peanut agglutinin (brown) and IgD (blue). Arrows indicate GCs. *G*, T cell-independent Ag (type II)-specific or TD-Ag-specific immune responses in *Ganp*^{Tg}. Sera from mice immunized with TNP-Ficoll or TNP-KLH were collected at day 14. TNP-specific Ab titers were measured by ELISA. C57BL/6 mice (●) and *Ganp*^{Tg} mice (○) are indicated. *H*, Relative affinity of serum Abs in *Ganp*^{Tg}. Sera from C57BL/6 and *Ganp*^{Tg} mice immunized with NP-CG were collected at days 14 and 28. The NP_2 to NP_{17} ratios of anti-NP IgG1 were measured by ELISA. *I*, W33L mutation of $V_H186.2$ transcripts from C57BL/6 and *Ganp*^{Tg} mice. Mice were i.p. immunized by 20 μg of alum-precipitated NP-CG. $V_H186.2$ transcripts of γ1-isotype were amplified by RT-PCR and cloned into pBluescript vector for sequencing. The calculated percentage from sequence data was shown in C57BL/6 (■) and *Ganp*^{Tg} (□) mice. *, $p < 0.05$.

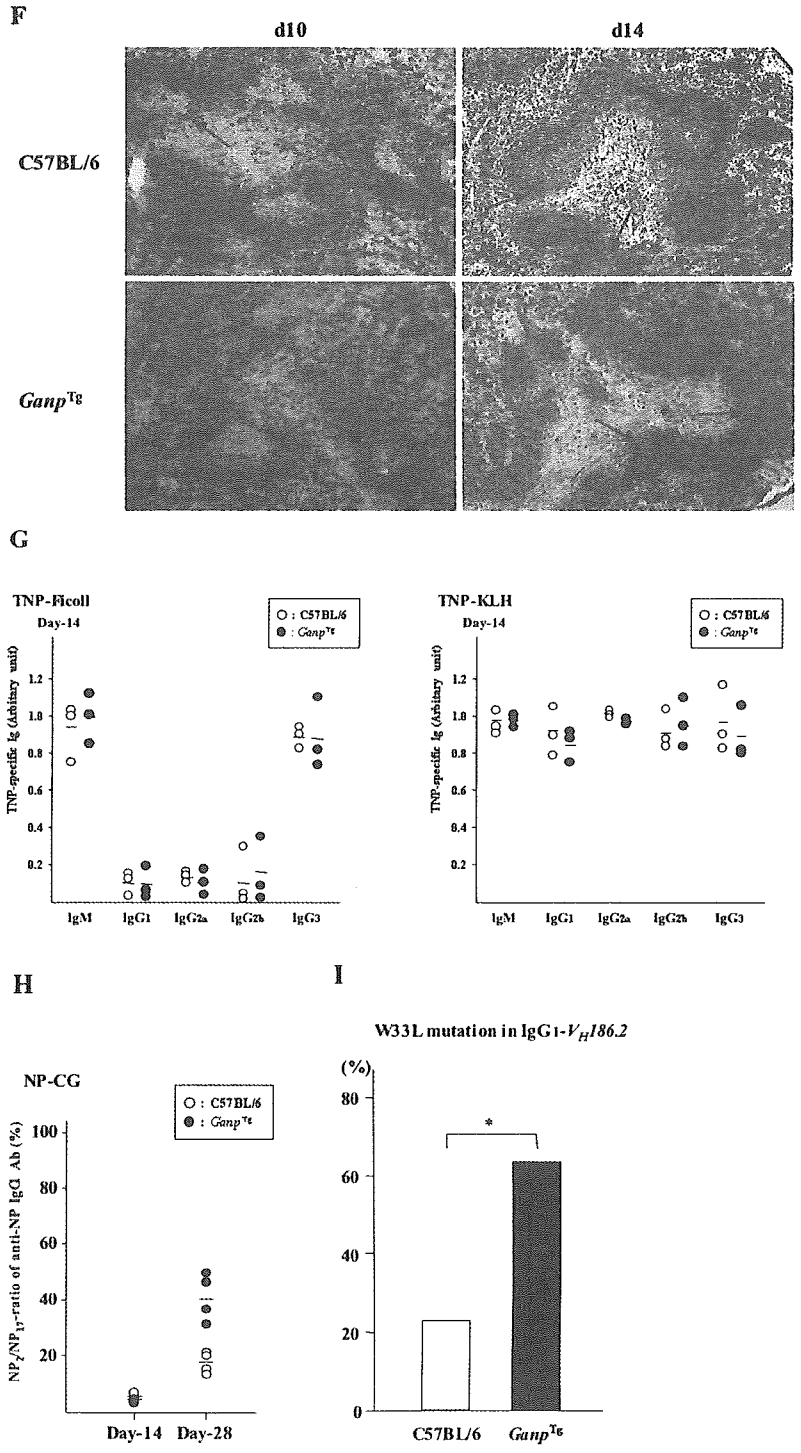

FIGURE 1. *continued.*

and incubated with anti-IgD mAb in combination with alkaline phosphatase-conjugated anti-rat IgG (ICN Pharmaceuticals). The first development step was conducted with Vector Blue kit (Vector Laboratories). For second staining, slides were incubated with biotin-conjugated peanut agglutinin (Vector Laboratories) in combination with HRP-conjugated streptavidin (Kirkegaard & Perry Laboratories), followed by 3,3′-diaminobenzidine tetrahydrochloride (Dojindo). After fixation with 1% glutaraldehyde in PBS, mounting was done by Aquatex (Merck).

Ag and immunization

2,4,6-Trinitrophenyl (TNP)-keyhole limpet hemocyanin (KLH), TNP-Ficoll, and NP_{28}-CG were purchased from Biosearch Technologies. From 20 to 100 μg of TNP-KLH and NP-CG precipitated by alum (Pierce), or 25 μg of TNP-Ficoll dissolved in PBS was injected i.p. into C57BL/6 and *Ganp*^{Tg} mice.

Measurement of Ag-specific Ab production

Five micrograms per well of TNP-BSA (Biosearch Technologies) were coated on ELISA plate, blocked with 3% BSA in PBS, and incubated with the serial-diluted sera obtained at day 14 after Ag immunization. After washing with PBS-0.1% Tween 20, the wells were incubated with biotin-conjugated isotype-specific mAb in combination with alkaline phosphatase-conjugated streptavidin (Southern Biotechnology Associates). The development was performed in the presence of substrate.

Sequence analysis of V_H186.2 gene

The *Ganp*^{Tg} mice were immunized with alum-precipitated NP-CG once as described (5). After 28 days, the spleen B cells were purified, and the total

Table I. *Affinity of the anti-NP mAb measured by BIAcore sensorgram*

mAb	H Chain	L Chain	V_H Usage	K_D, M[a]
Ganp^{Tg}				
NP-G2-6	γ1	κ	V_H 7183 family	7.05×10^{-8}
NP-G2-9	γ1	κ	V_H 7183 family	3.24×10^{-8}
NP-G2-12	γ1	λ	V_H 186.2	4.92×10^{-8}
NP-G2-14	γ1	κ	V_H 186.2	2.51×10^{-8}
NP-G2-16	γ2b	λ	V_H 186.2	1.10×10^{-7}
NP-G2-15	γ1	λ	V_H 186.2	4.12×10^{-8}
NP-G-2E4	γ2b	λ	V_H 186.2	1.57×10^{-9}
C57BL/6				
NP-W2-7	γ1	λ	V_H 186.2	1.51×10^{-7}
NP-W1-116	γ2a	λ	V_H 186.2	1.00×10^{-8}
NP-W-1B9	γ2b	λ	V_H 186.2	1.24×10^{-8}
NP-W-2D8	γ2b	λ	V_H 186.2	2.74×10^{-8}

[a] K_D was calculated using BIAcore sensorgram as described in *Materials and Methods*.

RNA was used for RT-PCR analysis with the sequence primers for IgG1-V_H*186.2* and the sequences were compared with those of C57BL/6.

Establishment of mAbs

Ag immunization was conducted with CFA as a primary immunization and then followed by boosting with IFA (4). For anti-NP-specific mAbs, NP_{28}-CG emulsified in CFA was injected i.p. and boosted after 2 wk with IFA. The mice with higher serum Ab titers were further immunized, and 3 days later, the spleen cells were obtained for cell fusion by polyethylene glycol method with mouse myeloma cell line X63 under the standard procedure (4). The fused cells were selected with hypoxanthine/aminopterin/thymidine medium on the microculture plates at the concentration of 2×10^4 cells/well with IL-6 (5 U/ml). For preparation of mAbs against the epitope of HIV-1, the peptide of the CNNTRKSIRIQRGPGRAFVYIGKI was prepared based on the amino acid sequence of the V3 loop of gp120 region of NL4-3 HIV-1 strain (prototype X4; T cell tropic) and conjugated with KLH (Merck). Sera of immunized mice were measured by ELISA using the plates coated with the HIV-1 peptide conjugated with BSA.

ELISA screening

For anti-NP mAbs, supernatants of individual wells were divided into two aliquots (each 50 μl) and measured by the differential ELISA method with two different Ag-coating as NP_2-BSA and NP_{17}-BSA (Biosearch Technologies) under the standard procedure. The mAbs binding to the Ags were captured with protein A-peroxidase (Amersham Biosciences) with the substrate (Bio-Rad). The positive signals with NP_2-BSA plates were selected in comparison with NP_{17}-BSA plates. The mAbs showing little difference (NP_2-BSA/NP_{17}-BSA > 0.5) between the two plates were cloned by limiting dilution method. Then, the positive clones were expanded for large scale to purify the mAbs in the serum-free medium (Invitrogen Life Technologies) and the mAbs were purified through protein G-Sepharose column chromatography (Amersham Biosciences) and the protein concentrations were determined by Bradford assay kit (Bio-Rad). The purities of the samples were examined by SDS-PAGE and the protein staining with Coomassie brilliant blue. The isotypes of H chain and L chain in all mAbs were determined by Isotyping kit (Dainippon Pharmaceuticals).

BIAcore assay

Affinity of the mAbs was determined by the BIAcore assay (7). The on and off rate constants (k_{on} and k_{off}) for binding of the mAbs to NP or HIV-1 V3 loop peptide were determined by BIAcore system (Biacore International). The carboxyl-methylated dextran surface of the sensor chip was activated with EDC (*N*-ethyl-*N'*-(3-dimethylaminopropyl)carbodiimide) and NHS (*N*-hydroxysuccinimide) (8). V3 loop peptide was immobilized through the free thiol group of a cysteine residue that was deliberately placed at the N terminus, by injection of 35 μl of a 20 μg/ml solution in 10 mM MES buffer (pH 6) to the EDC-NHS-activated surface that had been reacted with 2-(2-pyridinyldithio)ethaneamine. The excess disulfide groups were deactivated by the addition of cysteine. The mAbs were diluted in 10 mM HEPES (pH 7.4), 150 mM NaCl, 3.4 mM EDTA, and 0.05% (v/v) BIAcore surfactant P20 and injected over the immobilized Ag at a flow rate of 5 μl/min. The association was monitored by the increase of the refractive index of the sensor chip surface per unit time. The dissociations of the mAbs were monitored after the end of the association phase with a flow rate of 50 μl/min. Kinetic rate constants were calculated from the collected data using the Pharmacia Kinetics Evaluation software (9). The k_{on} was determined by measuring the rate of binding to the Ag at different protein concentrations.

DNA sequencing

The DNA fragments corresponding to the rearranged V_H regions were amplified using Pfu-Turbo (Stratagene) from the genomic DNA. The oligonucleotide primers are as follows (10, 11): V_H186.2 forward, 5'-CTGAC CCATGTCCCTTCTTCTCCAGCAGG-3'; V_H7183 forward, 5'-GCA GCTGGTGGAGTCTGG-3'; J_H4-3, 5'-CTCTCAGCCGGCTCCCTCA GGG-3'; Vλ1 forward, 5'-TGCTGACCAATATTGAAAAG-3'; Jλ1 reverse, 5'-AGCACCTCAAGTCTTGGAGAG-3'. For rearranged *V* κ-chain genes, the cDNA fragments were amplified using the primers designed as follows (12): V κ-Ox1 forward, 5'-ATGGATTTTCAAGTGCAGATTTTCA-3'; Vκ-21B forward, 5'-ATGGAGTCAGACACACTCCTGCTAT-3'; and Cκ reverse, 5'-TGGGAAGATGGATACAGTTGGTGCA-3'. Amplification of Cμ region was conducted with the primers: Cμ-Ex1 forward, 5'-AGTCAGTCCTTCCCAAATGTCTTCCC-3' and Cμ-Ex3 reverse, 5'-TGAAGGTTAGGATGTCTGTGGAGGG-3'. The amplified DNA fragments cloned into blunt-ended pBluescript were sequenced.

In vitro binding assay to NL4-3 envelope

293T cells were transfected with pLP-IRES2 enhanced GFP (BD Clontech) or pLP-NL4-3 envelope enhanced GFP using Effectene Transfection Reagent (Qiagen). After 36 h, cells were harvested, incubated with each anti-HIV-1 mAb in combination with allophycocyanin-conjugated goat anti-mouse IgG Ab (BD Pharmingen), and analyzed in comparison with GFP expression by FACSCalibur. The anti-CD19 mAb was purchased from BD Biosciences.

Neutralization activity assay

HIV-1 strain NL4-3 (prototype X4; T cell tropic) was propagated in PM1 cells in RPMI 1640 medium with 10% (v/v) heat-inactivated FCS, and the cell-free supernatant was collected and stored as virus stocks at −80°C. The chemiluminescent assay (Galacto-Star; Applied Biosystems) for β-galactosidase released from the HeLa-CD4$^+$/long terminal repeat (LTR)-β-galactosidase/CCR5 (MAGI/CCR5) cells were conducted as previously described (13). Tissue culture-effective dose $(TCID)_{50}$ of virus stock was predetermined with MAGI/CCR5 cells by the method of Reed and Muench (14). For the assay of neutralizing activity against HIV-1 infection, MAGI/CCR5 cells were plated in 96-well microtiter plates at a density of 1×10^4 cells/well, and on the next day, the cells were incubated with 50 μl of each mAb and 50 μl of HIV-1 solution (500 $TCID_{50}$) for 30 min at 37°C in combination with 10 μg/ml DEAE-dextran (Amersham Biosciences) in a triplicate assay. After 48 h, we measured the β-galactosidase activity for 1 s using the Galacto-Star system according to the manufacturer's protocol and showed results as percentages of the negative control.

Results

Establishment of Ganp^{Tg} *mice*

Ganp^{Tg} mice were established under control by human Ig enhancer and mouse Ig promoter in C57BL/6 background (Fig. 1, *A* and *B*), and the adult mice showed an increase of *ganp* transcripts (~2-fold) in B cells (Fig. 1*C*). *Ganp*^{Tg} mice had normal B lineage differentiation by surface marker studies of B220, IgM, and IgD on lymphoid cells in the bone marrow, spleen, and lymph nodes (Fig. 1*D*). B cell numbers and the levels of serum Igs were also normal in *Ganp*^{Tg} mice (data not shown). These results demonstrated that B cell differentiation undergoes normally in *Ganp*^{Tg} mice compared with wild-type littermates.

In vitro B cell proliferation and GC formation of Ganp^{Tg} *mice*

Next, we examined the potential of B cell proliferation of *Ganp*^{Tg} mice in vitro. *Ganp*^{Tg} mice showed comparable proliferation activities to wild-type littermates in response to anti-μ Ab, anti-μ Ab plus anti-CD40 mAb, or LPS (Fig. 1*E*). Interestingly, *Ganp*^{Tg} B cells showed augmented responses to anti-CD40 stimulation in comparison to wild-type B cells. This was only observed in the response to anti-CD40 stimulation but not in the response to anti-μ Ab or LPS stimulation, suggesting that *Ganp*^{Tg} mice augment CD40-stimulated response in vivo.

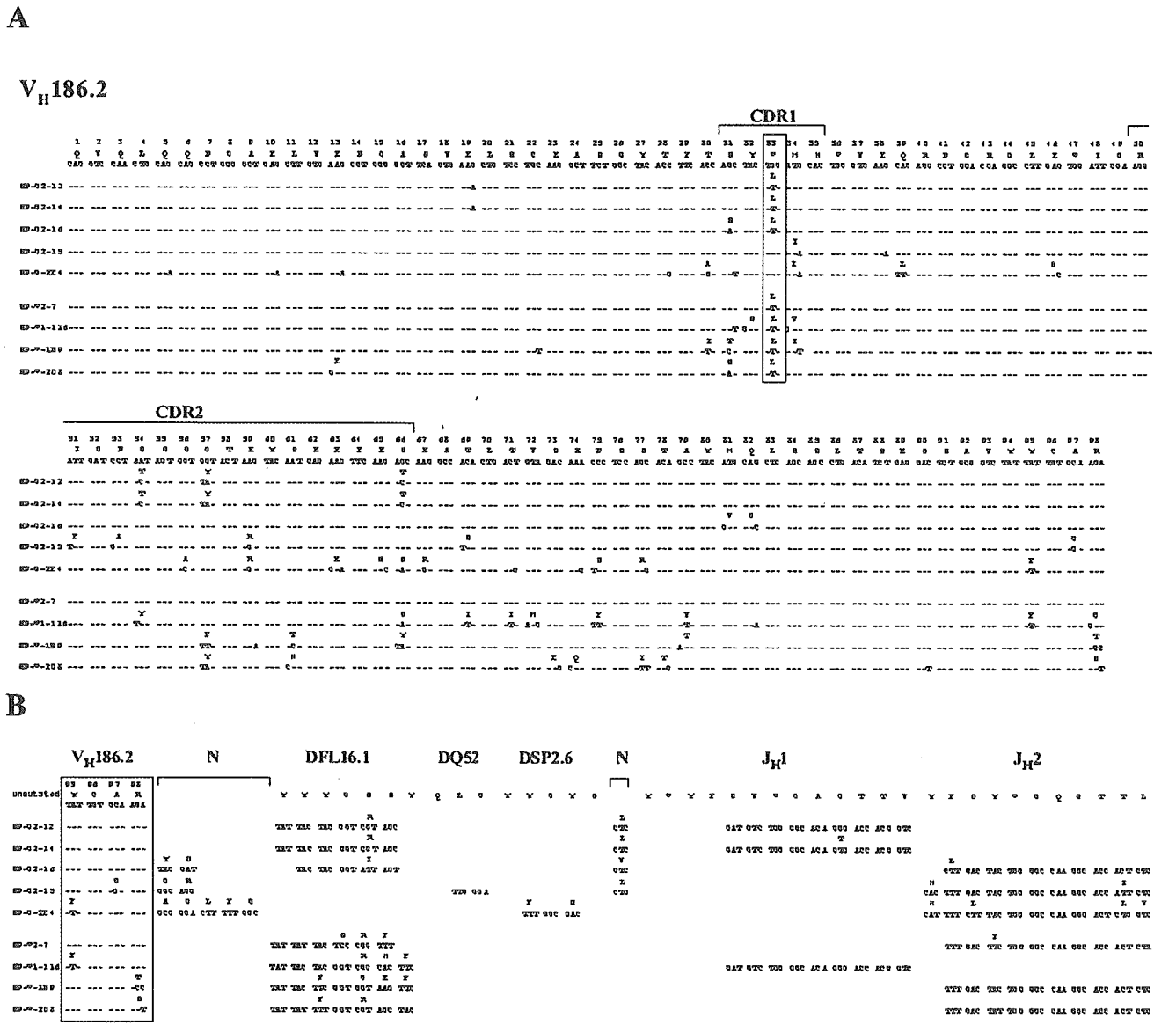

FIGURE 2. *(continues)*

We examined whether *Ganp*^{Tg} mice showed the alteration of GC formation in vivo. *Ganp*^{Tg} mice did not show any difference in the size and number of GCs at day 10 after SRBC immunization; however, in contrast to the findings observed in B-*ganp*$^{-/-}$ mice (4), *Ganp*^{Tg} mice showed the accelerated resolution of GC formation in vivo (Fig. 1*F*). This response could be due to the efficient production of high-affinity Ab in *Ganp*^{Tg} mice.

Responses of Ganp^{Tg} *mice against T cell-independent Ag and TD-Ag*

Because GANP expression is selectively up-regulated in GC B cells, we studied the Ab responses of *Ganp*^{Tg} mice. After Ag immunization, the responses were measured for T cell-independent type II Ag and TD-Ag at various time points and the results of day 14 were shown. The serum titers of Ag-specific Abs against TNP-Ficoll as T cell-independent Ag and TNP-KLH as TD-Ag were normal with similar distributions of various Ig isotypes in comparison with wild-type littermates (Fig. 1*G*).

Enhanced affinity maturation of Ganp^{Tg} *mice against TD-Ag*

However, after immunization with NP-CG, *Ganp*^{Tg} showed high affinity by the differential ELISA with the pauci NP_2-BSA conjugate that yielded 42% of the response to the multihapten NP_{17}-BSA conjugate in comparison with C57BL/6 (Fig. 1*H*). Jacob et al. (15, 16) showed that, in (NP-CG)-immunized C57BL/6 mice, the Abs in the secondary response against NP were exclusively IgG1/λ1 and had a single V_H region (V_H186.2) carrying with a peculiar pattern of mutation for high affinity. We investigated whether the affinity increase of anti-NP Ab generated in *Ganp*^{Tg} mice accompanied with the similar mutation pattern in the *V_H186.2* locus. The *V_H186.2* sequence was studied by RT-PCR using the spleen B cells from (NP-CG)-immunized mice. *Ganp*^{Tg} showed striking increases in mutation at ^{33}W to L of the *V_H186.2* locus in splenic B cells (W33L; Fig. 1*I*). These results demonstrated that *Ganp*^{Tg} induced a higher frequency of the high-affinity mutation during the immune response to TD-Ag.

Establishment of hybridomas secreting high-affinity anti-NP-hapten

Anti-NP hybridomas were established by immunization of *Ganp*^{Tg} with NP-CG. Supernatants from >6000 clones were screened by the differential ELISA to identify wells with high-affinity mAbs, and the selected hybridoma cells were cloned. Affinities of those

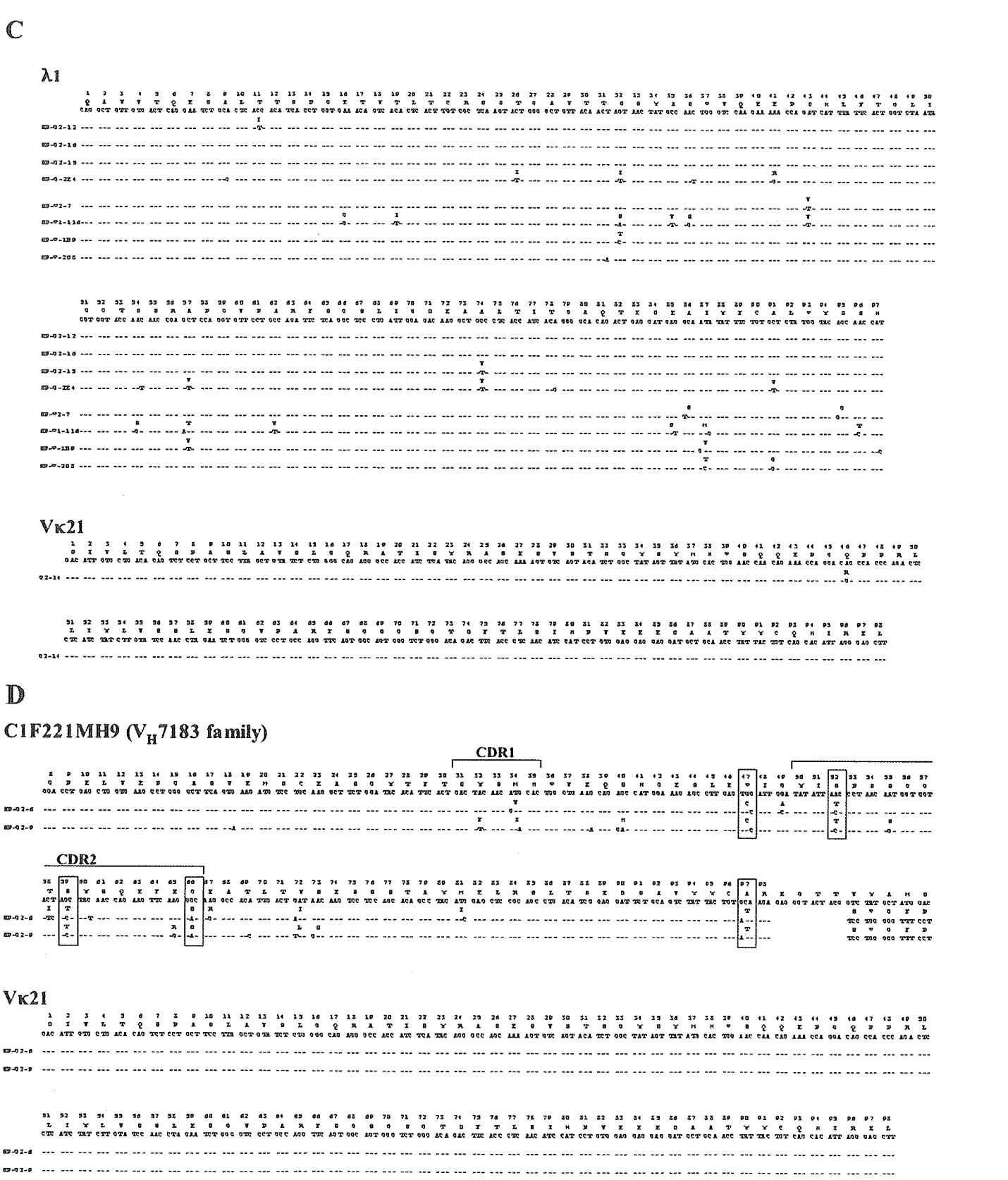

FIGURE 2. Sequence analysis of the *V* region genes of the hybridomas secreting anti-NP mAbs. V_H regions were determined using the primers commonly applicable to the major V_H families and the J_H4 primer (12). The individual *V* region sequence was determined after cloning of the genomic PCR products. Each sequence was determined by three sequencing reactions. *A*, The sequences of the clones using the V_H186.2 region are aligned and the site of W33L mutation is boxed. *B*, The sequences of the VDJ recombination regions are aligned. The part of the V_H186.2 region was boxed. *C*, The V_L region sequences were determined similarly to the method used for V_H regions. *D*, The sequences of the V_H and V_L regions of the two anti-NP mAbs that used noncanonical V_H regions are shown. The mutations shared between the two mAbs are boxed.

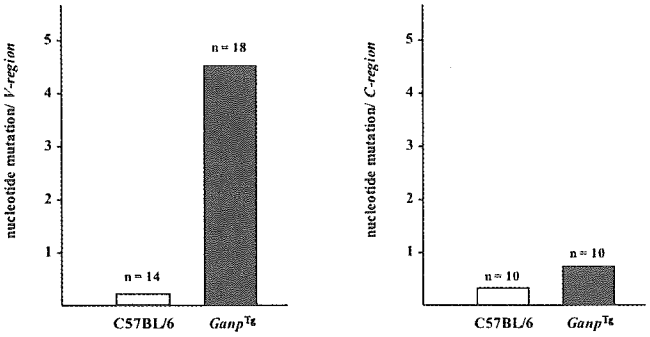

FIGURE 3. Mutation frequency induced in the V_H7183 family gene (C1F221MH9) by NP-CG immunization. NP-binding GC B cells were purified by a cell sorter 14 days after immunization with NP-CG in $Ganp^{Tg}$ and C57BL/6 mice. The V_H7183 family gene and $C\mu$ gene were PCR-amplified by Pfu-Turbo with genomic DNAs, cloned into TOPO cloning vector, and then sequenced. The mutation frequencies were counted based on the genomic sequences in the European Molecular Biology Laboratory database and were shown as average mutations per V_H region or $C\mu$ region sequences. The number (n) shows the V_H region (*left*) or $C\mu$ region (*right*) DNAs cloned in the TOPO cloning vector.

mAbs, after purification from clone culture supernatants, to NP-hapten were measured by the BIAcore system with a sensor chip conjugated with NP using Pharmacia Kinetics Evaluation software (9). The K_D of each mAb was determined by measuring the rate of binding to the Ag at different protein concentrations. The affinity of mAbs from (NP-CG)-immunized $Ganp^{Tg}$ and C57BL/6 mice were compared and the representatives were shown (Table I). The high-affinity mAbs of C57BL/6 mice used the $V_H186.2$ region in combination with λ1 L chain and yielded affinities from $K_D = 1.51 \times 10^{-7}$ M to 1.0×10^{-8} M. The mAbs from $Ganp^{Tg}$ showed the usage of canonical V_H186.2 in combination with both κ and λ yielding affinities from $K_D = 1.10 \times 10^{-7}$ M to 1.57×10^{-9} M. Interestingly, the mAbs from $Ganp^{Tg}$ also used noncanonical V_H region of V_H7183 family in combination κ-chain but showed similarly high affinities.

The usage and mutation of V *region genes in the anti-NP hybridomas*

The high-affinity mAbs obtained from C57BL/6 mice used the canonical $V_H186.2$ gene with the W33L mutation that is responsible for high affinity. This change increased the affinity from $K_D = 2 \sim 4 \times 10^{-6}$ M to 2×10^{-7} M (17, 18). The other mutations in the $V_H186.2$ gene segment would not have contributed to increased affinity against NP-hapten (19). Therefore, we sequenced the V_H regions of the hybridomas to examine whether there were similar mutation profiles of the V region. The mAbs from C57BL/6 mice generated typical high affinity against NP-hapten by using the $V_H186.2$ region with W33L mutation in combination with $DFL16.1$ and J_H2 gene segments. $Ganp^{Tg}$ generated similar high-affinity mAbs (NP-G2-12; $K_D = 4.92 \times 10^{-8}$, NP-G2-16; 1.10×10^{-7} M) (Table I) with the V_H186.2 having the W33L mutation (Fig. 2*A*). Interestingly, two anti-NP hybridomas that did not bear the W33L mutation in V_H186.2 showed similar high affinities. NP-G2-15 had the mutation of Y99G as reported previously (10). NP-G-2E4 with higher affinity ($K_D = 1.57 \times 10^{-9}$ M) did not have either of these two mutations but instead showed 13 aa mutations (22 nt changes) in the V_H186.2 region with the usage of DSP2.6 and J_H2 regions (Fig. 2, *A* and *B*). The L chain of NP-G-2E4 also had 6 aa mutations (10 nt changes) (Fig. 2*C*). This result suggested that the high affinity of NP-G-2E4 was generated by the extraordinarily increased V region mutations.

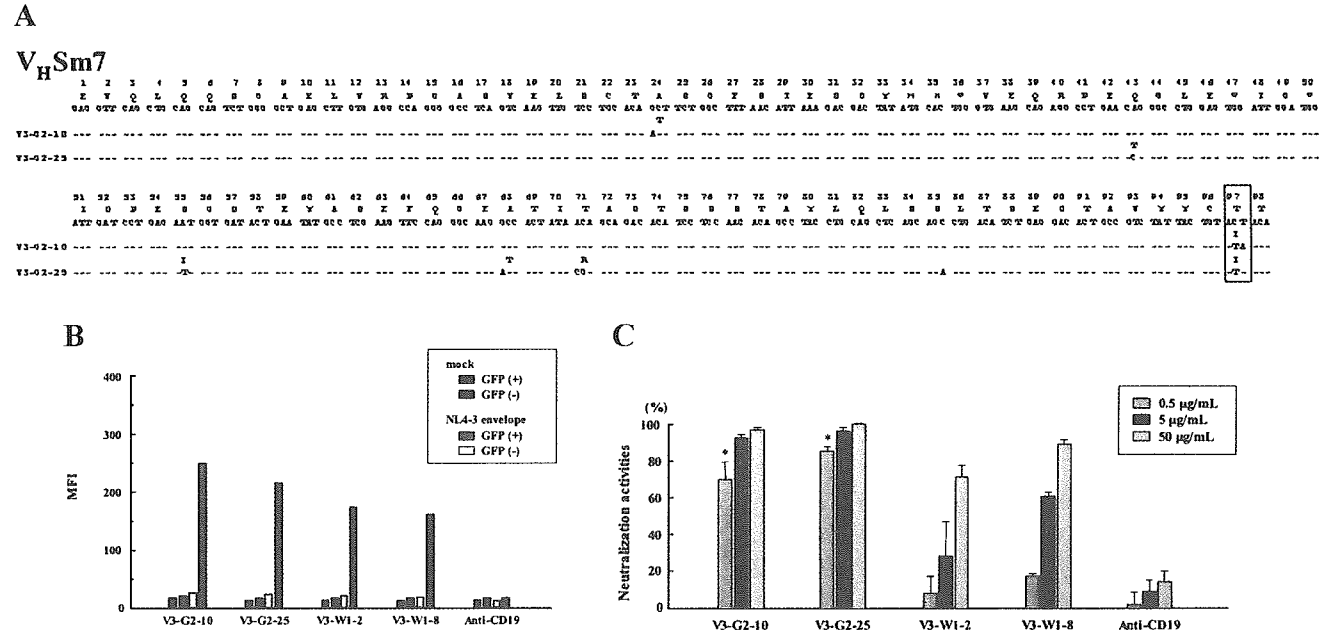

FIGURE 4. The sequences of the V_H region, the Ag-binding activities, and the neutralizing activities of the mAbs against the V3 epitope of HIV-1 gp120. *A*, The V_H region sequence (V_HSm7) used for the high-affinity mAbs from $Ganp^{Tg}$ is shown. The mutation site commonly observed in the two V_H sequences is boxed. *B*, Binding activity of the mAbs against HIV-1 envelope. Specific binding of the mAbs were shown as mean fluorescence intensity (MFI) examined with allophycocyanin-conjugated goat anti-mouse IgG Ab in combination with the NL4-3 envelope-expressing GFP^+-transfectants by using flow cytometry. Negative controls were measured with GFP^--mock transfectants. Another negative control for mAb binding was shown by CD19 mAb. *C*, Neutralizing activities were measured using a CD4-LTR/β-galactosidase-induced HeLa cell line. After $TCID_{50}$ of virus stock was predetermined with MAGI/CCR5 cells, the virus infection assay was conducted in vitro, to which anti-V3 epitope mAbs were added. Higher neutralization activities were significant (*) for the mAbs produced by $Ganp^{Tg}$ (V3-G2-10 and V3-G2-25) as compared with those of C57BL/6 mice at the concentration of 0.5 μg/ml. Negative control is shown with anti-CD19.

Moreover, two anti-NP mAbs from *Ganp*^{Tg} yielding similarly high affinities (K_D = 3.24 ~ 7.05 × 10^{-8} M) used noncanonical V_H region sequences, both of which probably originated from the same genomic *V_H7183* family. The best match in the Celera Discovery System was to the C1F221MH9 (*V_H7183* family), but the two clones showed variations with >12 nt differences from the genomic C1F221MH9 sequence (Fig. 2*D*). Mutations of W47C, N52C, S59T, G66D, and A97T were commonly observed in the V_H region (C1F221MH9), suggesting their contributions to raise the affinity of the mAb against NP-hapten. However, mutations in the V_L regions were not apparently increased in the comparison of the anti-NP mAbs from *Ganp*^{Tg} and C57BL/6 mice. The generation of high-affinity BCR without the exchange at position 33 is a rare event, which suggested that the combination of particular D-J_H sequences and/or many SHMs do not result in high affinity (18). A recent report only showed the case of mutation, Y99G in V_H186.2, which generated similar high-affinity mAb against NP-hapten comparable to W33L (10). Extensive earlier studies of anti-NP mAbs found that repeated immunization of C57BL/6 mice with NP-CG increased usage of noncanonical V_H regions and different L chain combinations (16). However, as far as we know, no study with conventional animals has demonstrated comparable high-affinity mAbs to those reported in this study. Although crystallographic studies are needed for definitive conclusions, we speculate that hypermutated C1F221MH9 V_H region (V_H7183 family) in association with other L chain combinations creates an effective tertiary structure for Ag-binding, yielding closer interactions of hypermutated C1F221MH9 V_H region and NP-hapten, and might be as effective as mAbs with the V_H186.2 region.

Mutations induced in the noncanonical V_H region of the spleen B cells after immunization with NP-CG

Usually wild-type C57BL/6 mice do not induce such a frequent mutation in the noncanonical V_H region in GC B cells before and after immunization with NP-CG. We examined the mutation frequency of the *V_H7183* family gene (C1F221MH9) under a non-immunization condition in spleen B cells of *Ganp*^{Tg} mice but found no alteration of the *V_H* region (data not shown). To study whether such hypermutation could be observed in *Ganp*^{Tg} spleen B cells after immunization, we investigated mutations in the *V_H7183* family gene (C1F221MH9) by examining genomic DNA of NP-binding GC B cells purified by cell sorting. These DNAs showed 16-fold higher mutation frequencies (4.5 mutations/*V_H* region of *Ganp*^{Tg} mAb vs 0.28 mutations/*V_H* region of C57BL/6 mAb) in the *V_H7183* family (Fig. 3, *left panel*). In contrast, such higher mutation frequencies were not observed in the Cμ region (Fig. 3, *right panel*). This is in agreement with the suggestion that *Ganp*^{Tg} has a high frequency of SHM that contributes to the production of high-affinity BCR in vivo. Alternatively, *Ganp*^{Tg} might effectively rescue and maintain B cells with high-affinity BCR during the immune response.

Establishment of high-affinity mAbs against HIV-1 by use of Ganp^{Tg} *mice*

To apply this system for generating high-affinity Ab using *Ganp*^{Tg} mice, we studied whether high-affinity anti-HIV-1 mAbs with significant neutralization activity against virus infection could be generated by immunization with the V3 loop peptide (NL4-3) of HIV-1 gp120. Differential ELISA using plates coated with high and low doses of the V3 peptide initially identified hybridoma cells with relatively high-affinity mAbs from >6000 wells of (V3 peptide)-immunized *Ganp*^{Tg} and C57BL/6 mice. High-affinity clones were selected from each mouse strain. After further cloning, individual mAbs were purified and their affinities were measured using the BIAcore system. The mAbs from both mouse systems showed higher affinities in a range from K_D = 2.81 × 10^{-5} M to ~ 5.67 × 10^{-9} M. However, we could obtain extraordinarily higher affinity mAbs (V3-G2-10 and V3-G2-25; K_D = 9.90 × 10^{-11} M) from *Ganp*^{Tg} over the level that is generally not attainable by conventional methods of mAb preparation (20). The highest affinity mAbs (V3-W1-2 and V3-W1-8) from C57BL/6 mice were up to K_D = 9.81 × 10^{-8} M and 7.58 × 10^{-8} M. The high-affinity mAbs from *Ganp*^{Tg} used the same V_H region (V_HSm7) with the common mutation at T97I, suggesting that the T97I mutation contributed to an affinity increase against the V3 epitope (Fig. 4*A*). A binding assay involving HIV-1 envelope (NL4-3) gene-transfected cells was used to determine whether the mAb recognized the viral epitope. The binding activities to the transfectants were studied by flow cytometry as mean fluorescence intensity in comparison with the GFP-positivity as indicators of gene transfection. The mAbs (V3-G2-10, V3-G2-25, V3-W1-2, and V3-W1-8) showed higher binding activities to the virus epitope-expressing cells (Fig. 4*B*).

The neutralization activities of these anti-HIV-1 mAbs were examined using a CD4-LTR/β-galactosidase-transduced HeLa cell line that expresses high levels of human CD4 and contains a single integrated copy of a *β-galactosidase* gene under the control of a truncated HIV-1 LTR (13, 21). Neutralization activities of the two high-affinity mAbs (V3-G2-10 and V3-G2-25) were clearly detected at 0.5 μg/ml, which were more effective than those of mAbs (V3-W1-2 and V3-W1-8) from C57BL/6 (Fig. 4*C*). The simple comparison might indicate 50–100 times increase of affinity in the mAbs from *Ganp*^{Tg} mice. These mAbs with high-affinity Ag-binding and neutralization activities should be useful for clinical diagnostic purposes and analogous human mAbs might have therapeutic possibilities (22).

Discussion

Expression of GANP is required for generation of high-affinity Ab response in vivo, which was demonstrated by conditional targeting of *ganp* gene in B cells that caused apparent decrease in production of high-affinity Ab against NP-hapten, accompanied with the decreased frequency of high-affinity type mutation of W33L at the V_H186.2 in NP-binding IgG1$^+$ B cells (5). Several possibilities might be considered to explain the mechanism of GANP in generation of high-affinity BCR$^+$ B cells in vivo. GANP might be directly linked in genetic alteration, including *V* region dsDNA breaks occurring in B cell proliferation (23), SHM events in association with activation-induced cytidine deaminase (24), uracil DNA glycosylase (25), and error-prone DNA polymerases up-regulated in GC B cells (26), DNA recombination and repair mechanisms or rather involved in the selection of high-affinity BCR$^+$ B cells in the follicular dendritic cell network (27), and survival and maintenance of B cells with high-affinity type mutations throughout the immune response.

There are several possible mechanisms regarding the GANP function. Firstly, GANP might directly regulate generation of mutation frequency of the V_H region in GC B cells. The structure and expression of GANP indicated that GANP has two nuclear localization signal sequences (^{497}HKKK and ^{1344}PMKQKRR), two putative nuclear export signal sequences, and appears mostly in the nucleus but is also in the cytoplasm (our unpublished observation). The C-terminal region is capable of binding and acetylating with MCM3 of the MCM-complex that bears DNA helicase activity and is essential for DNA replication (28). In the N-terminal side, there is a putative RNA-associated region as the RNA recognition motif. The RNA-primase region and the RNA-binding activity might cooperate during the transcription at G_1 phase and introduce the alteration or the damage of the *V_H* region sequences during rapid cell proliferation in GCs. More interestingly, altered expression of

mouse SHD1 that has a homology to the central part of GANP (630–950 aa) caused an apparent cell cycle abnormality involving with centrosome duplication and M phase transition (29), which was also in accordance with the information of the association of *Saccharomyces* Sac3 with Cdc31/centrin (30). Loss of SHD1 caused an impairment of centrosome duplication, deregulated nuclear division, with disappearance of Mad2 expression in the prometaphase. Because mouse GANP is considered as a homologue of *Saccharomyces* Sac3 (31), GANP might be also involved in the centrosome duplication or the chromatin segregation during cell division. These observations suggested the involvement of GANP in either one or several mechanisms of gene transcription, DNA replication, and chromatin separation and cell division. Loss of GANP caused the increased apoptotic cells in GCs after immunization with TD-Ags (4), whereas the gain of function did not show obvious difference (data not shown). Second, these functions of GANP regions might be involved in the repair of DNA injuries occurring under a transcription-coupled mechanism or in the DNA replication phase. If this is the case, existence of GANP is critical for maintenance of DNA stability during the GC B cell stage that undergoes genetic alteration with frequent SHM of the V_H region and class switch recombination. Expression of GANP is necessary for the rescue of damaged GC B cells that potentially gain the high-affinity BCR. Third, additional function of GANP might be involved in generation or selection of high-affinity BCR^+ B cells in GCs. $Ganp^{Tg}$ mice showed accelerated kinetics of GC formation (Fig. 1*F*), whereas B-$ganp^{-/-}$ mice showed retarded GC formation (4). Recently, Mirnics et al. (32) described that GANP is involved in downstream event(s) of Lyn. As Lyn is involved in CD40-mediated signal transduction (33) and Lyn-deficient mice showed lack of GCs (34), there might be functional interaction of CD40-mediated signaling with the GANP function involved in regulation of high-affinity B cells. The augmented anti-CD40 response of $Ganp^{Tg}$ mice might support this notion, in which GANP is necessary for the rescue of high-affinity B cells during the selection in GCs. As a potential role of GANP in the selection process, GANP associates with a protein phosphatase component G5PR that associates with protein phosphatase 5 and protein phosphatase 2A (35). The complex of GANP with G5PR may regulate the other signaling pathways involved in cell survival mechanism or in regulation of BCR-mediated cell proliferation during maturation and selection of GC B cells. We have no definitive evidence to conclude the molecular mechanism at present but GANP is most likely a key molecule to elucidate the molecular mechanism in generation of high-affinity Ab in vivo.

To confirm the effect of GANP in generation of high-affinity Ab, we used a system to compare the affinity of the Abs at the monoclonal level by establishing the mAb-producing hybridomas. Affinity measurement with NP-hapten clearly demonstrated the high affinity of the mAbs generated from the $Ganp^{Tg}$ mice. Sequence analyses of the *V* regions of individual mAb-producing hybridomas demonstrated that the high affinity was generated not only with increased SHM frequency in the $V_H186.2$ region but also with the noncanonical V_H region usage that was not seen in the control hybridomas.

The results of both the loss and gain of GANP expression caused adverse effects in generation of high affinity response, which confirmed that the GANP function is involved in generation of high-affinity Ab in vivo. Additionally, the high-affinity is generated with the genetic alteration of *V* region genes as increased SHM and the different *V* region usage. GANP function might be directly involved in the formation of high affinity V region of the GC B cells. GANP is not up-regulated in the nonimmunized condition and is not expressed in normal T cells at the similar level detected with anti-GANP mAb (3). We speculate that up-regulation of GANP is selective in the cells with frequent genetic alterations such as *V* region SHM and class switch recombination during rapid proliferation phase.

In summary, we have demonstrated that $Ganp^{Tg}$ induces higher affinity Ab against TD-Ag in vivo, which was confirmed by BIAcore system with the purified mAbs against two model Ags of NP-hapten and the gp120 V3 peptide of HIV-1 by immunizing as TD-Ag. More importantly, the usage and the mutations of the V regions demonstrated that increased expression of GANP caused the genetic alteration of the *V* regions with increased mutations generating high affinity against TD-Ag in vivo. The results suggest that the $Ganp^{Tg}$ mouse has an advantage in preparation of mAbs against various epitopes, for which conventional mice hardly generate high-affinity mAbs by the standard procedures. High-affinity mAbs generated this way show greater epitope binding constants and this binding is long-lasting as measured in vitro. It would be useful to generate high-affinity mAbs against various molecules, which can be applicable widely in the diagnostic and therapeutic purposes.

Acknowledgments

We appreciate Dr. Y. Takahashi and Dr. T. Takemori for helpful advice and Y. Kumamoto for technical assistance.

Disclosures

The authors have no financial conflict of interest.

References

1. MacLennan, I. C. M. 1994. Germinal centers. *Annu. Rev. Immunol. 12:117.*
2. Rajewsky, K. 1996. Clonal selection and learning in the antibody system. *Nature 381:751.*
3. Kuwahara, K., M. Yoshida, E. Kondo, A. Sakata, Y. Watanabe, E. Abe, Y. Kouno, S. Tomiyasu, S. Fujimura, T. Tokuhisa, et al. 2000. A novel nuclear phosphoprotein, GANP, is up-regulated in centrocytes of the germinal center and associated with MCM3, a protein essential for DNA replication. *Blood 95:2321.*
4. Kuwahara, K., S. Tomiyasu, S. Fujimura, K. Nomura, Y. Xing, N. Nishiyama, M. Ogawa, S. Imajoh-Ohmi, S. Izuta, and N. Sakaguchi. 2001. Germinal center-associated nuclear protein (GANP) has a phosphorylation-dependent DNA-primase activity that is up-regulated in germinal center regions. *Proc. Natl. Acad. Sci. USA 98:10279.*
5. Kuwahara, K., S. Fujimura, Y. Takahashi, N. Nakagata, T. Takemori, S. Aizawa, and N. Sakaguchi. 2004. Germinal center-associated nuclear protein contributes to affinity maturation of B cell antigen receptor in T cell-dependent responses. *Proc. Natl. Acad. Sci. USA 101:1010.*
6. Koike, M., Y. Kikuchi, A. Tominaga, S. Takaki, K. Akagi, J. Miyazaki, K. Yamamura, and K. Takatsu. 1995. Defective IL-5-receptor-mediated signaling in B cells of X-linked immunodeficient mice. *Int. Immunol. 7:21.*
7. Jonsson, U., L. Fagerstam, B. Ivarsson, B. Johnsson, R. Karlsson, K. Lundh, S. Lofas, B. Persson, H. Roos, I. Ronnberg, et al. 1991. Real-time biospecific interaction analysis using surface plasmon resonance and a sensor chip technology. *BioTechniques 11:620.*
8. Johnsson, B., S. Lofas, and G. Lindquist. 1991. Immobilization of proteins to a carboxymethyldextran-modified gold surface for biospecific interaction analysis in surface plasmon resonance sensors. *Anal. Biochem. 198:268.*
9. Karlsson, R., A. Michaelsson, and L. Mattsson. 1991. Kinetic analysis of monoclonal antibody-antigen interactions with a new biosensor based analytical system. *J. Immunol. Methods 145:229.*
10. Furukawa, K., A. Akasako-Furukawa, H. Shirai, H. Nakamura, and T. Azuma. 1999. Junctional amino acids determine the maturation pathway of an antibody. *Immunity 11:329.*
11. Chen, J., P. Borden, J. Liao, and E. A. Kabat. 1992. Variable region cDNA sequences of three mouse monoclonal anti-idiotypic antibodies specific for anti-$\alpha_{1\text{—}6}$ dextrans with groove- or cavity-type combining sites. *Mol. Immunol. 29:1121.*
12. Wei, C., R. Zeff, and I. Goldschneider. 2000. Murine pro-B cells require IL-7 and its receptor complex to up-regulate IL-7Rα, terminal deoxynucleotidyltransferase, and cμ expression. *J. Immunol. 164:1961.*
13. Kimura, T., K. Yoshimura, K. Nishihara, Y. Maeda, S. Matsumi, A. Koito, and S. Matsushita. 2002. Reconstitution of spontaneous neutralizing antibody response against autologous human immunodeficiency virus during highly active antiretroviral therapy. *J. Infect. Dis. 185:53.*
14. Reed, L. J., and H. Muench. 1938. A simple method of estimating fifty percent end points. *Am. J. Hyg. 27:493.*
15. Jacob, J., G. Kelsoe, K. Rajewsky, and U. Weiss. 1991. Intraclonal generation of antibody mutants in germinal centres. *Nature 354:389.*
16. Jacob, J., J. Przylepa, C. Miller, and G. Kelsoe. 1993. In situ studies of the primary immune response to (4-hydroxy-3-nitrophenyl)acetyl. III. The kinetics of